European Gas Infrastructure Expansion Planning: An Adaptive Robust Optimization Approach

Iegor Riepin[a,*], Matthew Schmidt[b], Luis Baringo[c], Felix Müsgens[a]

[a] *Brandenburg Technical University, Chair of Energy Economics, Cottbus, Germany*
[b] *TU Dresden, Chair of Energy Economics, Dresden, Germany*
[c] *Universidad de Castilla-La Mancha, Escuela Técnica Superior de Ingeniería Industrial, Ciudad Real, Spain*

Abstract

The European natural gas market is undergoing fundamental changes, fostering uncertainty regarding both supply and demand. This uncertainty is concentrated in the value of strategic infrastructure investments, e.g., projects of common interest supported by European Union public funds, to safeguard security of supply. This paper addresses this matter by suggesting an adaptive robust optimization framework for the problem of gas infrastructure expansion planning that considers long-term uncertainties. This framework confronts the drawbacks of mainstream methods of incorporating uncertainty in gas market models (i.e., stochastic scenario trees), in which the modeler predefines the probabilities and realization paths of unknown parameters. Our mathematical model endogenously identifies the unfortunate realizations of unknown parameters, and suggests the optimal investments strategies to address them. We use this feature to assess which infrastructure projects are valuable in maintaining system resilience amid cold-winter demand spikes, supply shortages, and budget constraints. The robust solutions point to consistent preferences for specific projects. We find that real-world construction efforts have been focused on the most promising projects from a business perspective. However, we also find that most projects of common interest are unlikely to be realized without financial support, even if they would serve as a hedge against stresses in the European gas system.

Keywords: Adaptive robust optimization, Capacity planning, European gas market, Uncertainty

1. Introduction

Natural gas is a key energy source in modern economies, as it is used for heating, for generating electricity, and as a combustion fuel for industrial processes. Despite increasing global demand, recent years have seen the production of natural gas steadily decline in traditional European supply countries, such as Norway, the Netherlands, and the U.K. Hence, European dependence on natural gas is set to rise alongside rising competition for foreign resources. These two simultaneous developments entail heightened geopolitical risks,

*Corresponding author
Email addresses: iegor.riepin@b-tu.de (Iegor Riepin), matthew.schmidt@tu-dresden.de (Matthew Schmidt), luis.baringo@uclm.es (Luis Baringo), felix.muesgens@b-tu.de (Felix Müsgens)

25 October 2021

potentially triggering supply disruptions (IEA, 2019). While gas demand in Europe is expected to drop dramatically in the long term—under the assumption that policy objectives will be met—its trajectory in the medium term is subject to significant uncertainty, with scenarios anticipating a peak in 2030 (Fulwood, 2021). This uncertainty poses planning challenges for the European transmission system.

Since the initial foray of European Union (EU) into energy market liberalization, the issue of supply security has been a priority on the policy agenda (Smeers, 2008). The EU has proactively sought to enhance its infrastructural capacity in order to curb vulnerabilities. An official European energy security strategy instituted in 2014 tackles two policy priorities: first, boosting the short-term resilience of the natural gas network as a mechanism against supply interruption; second, reducing dependence on prevailing suppliers in the long term (European Commission, 2014). Policy-makers have lent great importance to heightening supply security through the development of new gas pipelines and liquefied natural gas (LNG) receiving terminals. European "projects of common interest" (PCIs) have been supported by public funds to advance market reform and further integrate and strengthen transnational gas infrastructure. Recently, these projects have been the target of significant criticism, with some arguing that they are unnecessary from a supply security perspective and are at risk of becoming stranded assets (Artelys, 2020).

In order to evaluate the impacts of uncertainties on European natural gas infrastructure and assess which infrastructure projects are critical to maintaining system resilience, this paper employs a adaptive robust optimization (ARO) approach (Bertsimas et al., 2013a,b). Several features of ARO make it particularly suitable for this purpose. First, ARO does not rely on the assumption of a finite number of uncertainty realizations with respective (known) probabilities. This feature confronts the drawbacks of mainstream methods of incorporating uncertainty in gas market models (i.e., stochastic scenario trees based on discrete probability distributions) (Birge and Louveaux, 2011; Yue et al., 2018). ARO requires only basic information about underlying uncertainty (e.g., the range of the uncertain data). Second, ARO is preferable when solutions exhibit strong sensitivity to minor changes in assumptions or input data. This feature is valuable in systems like the European natural gas market with complex spatial and intertemporal dynamics and numerous infrastructure assets. Finally, ARO has gained attention as a mechanism with which to model uncertainty in applications with high reliability requirements. Solution robustness in the context of energy systems is extremely valuable, as the penalty associated with infeasible solutions is exorbitant (Bertsimas et al., 2013b).

This paper addresses the following research questions:

- How can an adaptive robust optimization approach be employed to assess the impact of supply and demand uncertainties on infrastructure development in the European gas market?
- What implications do different levels of uncertainty have on specific infrastructure projects in the context of supply security?

ARO has gained prominence in the field of electricity systems analysis; however, in the field of gas network modeling, the applications has largely been restricted to testing distribution networks and stationary models (Cong et al., 2018; Aßmann et al., 2019). This paper contributes to the extant literature by applying ARO to model uncertainties in a real-world setting. To the best of our knowledge, this constitutes the first application of ARO in gas infrastructure expansion planning. Furthermore, we make an empirical contribution to the literature by assessing the implications of demand and supply uncertainty in 2030 on European natural gas

infrastructure.

To facilitate transparency and encourage future research in this field, the source code of the model and the associated input data for each scenario is published in a public GitHub repository: github.com/Irieo/ARO-GasInfrastructure. The code reproduces the results presented in the paper.

The remainder of the paper is organized as follows. Section 2 provides a brief overview of the methods used in this paper. Section 3 presents the formulation of the adaptive robust optimization problem, a representation of the employed uncertainty sets, and their empirical application to the European natural gas market. Section 4 reports and discusses the results and their implications. Section 5 concludes the paper with a summary of our analysis and a brief outlook on the potential for future research. Appendix A provides the detailed formulation of the adaptive robust optimization model for gas infrastructure expansion planning. Appendix B provides an illustrative example of the worst-case demand and supply realisations subject to uncertainty budgets. Appendix C lists projects of common interests included in our analysis. Appendix D complements literature review section and lists research papers that focus on natural gas markets and address parametric uncertainty.

2. Literature review

This section briefly reviews common approaches to model long-term uncertainties in the extant literature. In Section 2.1, we discuss methods for addressing long-term uncertainty in energy system models. In Section 2.2, we narrow our focus to natural gas market models.

2.1. Methods for addressing long-term uncertainty in energy systems models

The subject of long-term uncertainty in the context of model-based policy analysis has been vigorously discussed in the academic literature for decades (Lempert et al., 2003). Assessments of the impact of long-term systematic uncertainty in energy systems models commonly employ one of the three methods illustrated in Figure 1.

The vast majority of analyses incorporate uncertain parameters via deterministic scenarios (Figure 1a), often coupled with ex-post sensitivity analyses (Junne et al., 2019).

Another prominent method of incorporating uncertainty involves multi-stage stochastic optimization (Figure 1b). In this method, uncertain information is modeled by scenario trees (i.e., sequences of observable data vectors over the planning horizon). The branches (possible realizations of uncertain data) follow a probability distribution, which is assumed to be known to the decision-maker. At each stage, a decision must be irrevocably fixed based on the currently available information. One drawback of applying stochastic optimization to real-world problems is the fact that the realization probabilities of the random variables are mostly unknown (Kall and Wallace, 1994). Detailed reviews of the use of stochastic methods in energy system modeling are available in Wallace and Fleten (2003), Möst and Keles (2010), and Collins et al. (2017). However, a simple stochastic representation of uncertainty is not always viable when the probabilities of possible events are uncertain, knowledge of all possible events (unknown unknowns and black swans) is unavailable (Aven, 2013), or uncertainty is not purely exogenous.

The third method employs robust optimization (Figure 1c), which dates back to Soyster (1973). An adaptive robust optimization implements different techniques to improve on the original static robust optimization by incorporating multiple stages of decision into the algorithm (Zeng and Zhao, 2013). As noted

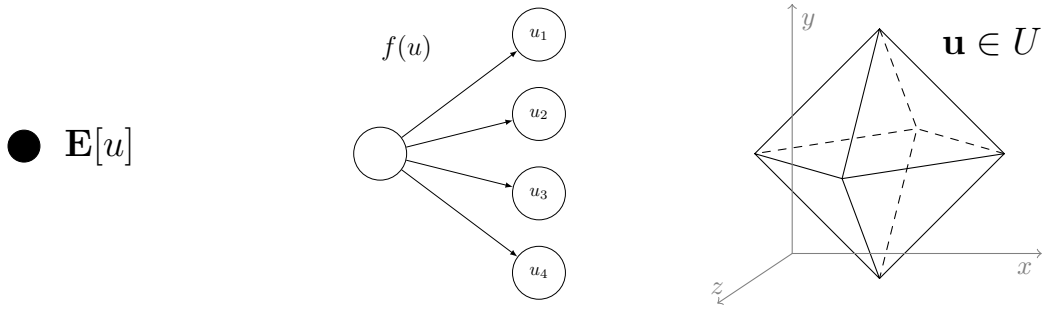

(a) Point estimate (deterministic) (b) Scenario tree (stochastic) (c) Uncertainty sets (robust)

Figure 1: Methods for incorporating uncertainty in energy optimization problems. Source: Authors' illustration

above, ARO is well-suited for applications where distributional information about a given uncertainty is limited or where solution feasibility is the ultimate evaluation metric. ARO renders solutions that exhibit feasibility for all possible realizations of uncertainty within a range defined in an uncertainty set. The set should be constructed to capture correlations among certain parameters. Although one can derive such sets based on probabilistic data, well-defined probability distributions are not required to construct uncertainty sets. Various types of uncertainty sets (e.g., box, polyhedral, ellipsoidal, cardinality-constrained budgets) have been employed in the extant literature (Lappas and Gounaris, 2018). Original box-type uncertainty sets were only able to accommodate the most conservative uncertainty manifestations. More recently, polyhedral uncertainty sets have been developed and employed (Bertsimas et al., 2011). Their uncertainty budgets can constrain the degree of uncertainty attached to a parameter. An in-depth review of its applications and methodological foundations can be found in Yanikoglu et al. (2019). In terms of its applications in the analysis of energy systems, ARO has been utilized to evaluate both short- and long-term uncertainties. Short-term analyses predominantly focus on electricity markets with unit commitment problems under uncertainty (e.g., intermittent wind power feed-in) (Bertsimas et al., 2013b; Zhou et al., 2018). Fewer short-term analyses involve natural gas, and most that do focus on scheduling problems in coupled electricity and gas markets (e.g., (Yao et al., 2018; Cong et al., 2018)). In terms of long-term uncertainties, a substantial strand of literature has applied variations of ARO to transmission-expansion planning models (e.g., (Ruiz and Conejo, 2015; García-Bertrand and Mínguez, 2017; Baringo and Baringo, 2018; Baringo et al., 2020)). There have yet to be any such ARO approaches to gas market modeling.

2.2. Long-term uncertainty and its representation in natural gas models

The subject of medium- to long-term uncertainty in natural gas markets has received considerable attention. The prevailing strand of analysis is deterministic in nature, deploying scenario and sensitivity analyses or (n-1) stress tests to incorporate uncertainty. More recently, model-based analyses have begun to adopt a stochastic approach in order to handle ranges of uncertain manifestations of relevant parameters (e.g., (Egging, 2013; Fodstad et al., 2016; Hauser, 2021; Riepin et al., 2021)). A tabular overview of such studies and their individual structures and representations of uncertainties is provided in Table D.1 in Appendix D.

The overview highlights that extant literature has explored developments in natural gas supply and demand. Prospective demand trajectories, supply interruptions, and infrastructural bottle-necks have been

in the focus of recent work. Research on the European market has focused on supply interruptions and infrastructure resilience on account of past geopolitical discord associated with transit negotiations regarding Russian gas supplied via Ukraine Abada and Massol (2011); Dieckhoener (2012); Egging and Holz (2016); Holz et al. (2016); Baltensperger et al. (2017); Hauser (2021). Given the uncertainty on the use of natural gas in medium-term trajectory, the prudence of impending investments in the resource remains in center of researchers' attention.

Our analysis contributes to the growing literature on this subject by employing a novel methodological approach to evaluate the resilience of European natural gas infrastructure under the worst-case combinations of uncertain demand and supply developments.

3. Problem formulation

This section details the formulation of the ARO model. For the sake of clarity, we first introduce an ARO problem in a compact form in section 3.1. Afterward, in section 3.2, we present a decomposition algorithm for the ARO problem. Finally, we apply the ARO model to a gas infrastructure expansion planning problem in section 3.3. In this section, we also parameterize the problem with the respective input data for the European natural gas market.

3.1. Compact formulation

The methodology takes stock of the ARO problems developed for energy markets (primarily electricity markets) (Baringo et al., 2020; Chen, 2016; Jabr, 2013; Mínguez and García-Bertrand, 2016; Ruiz and Conejo, 2015). These problems are formulated as three-level optimization problems. The robust problem can be written in compact matrix form, as illustrated in Figure 2.

The problem in Figure 2 includes three nested optimization layers:

1. The first level represents a planning strategy prior to the uncertainty realization (i.e., binary variables in vector x representing investment in transmission infrastructure projects with an investment cost vector C_I).

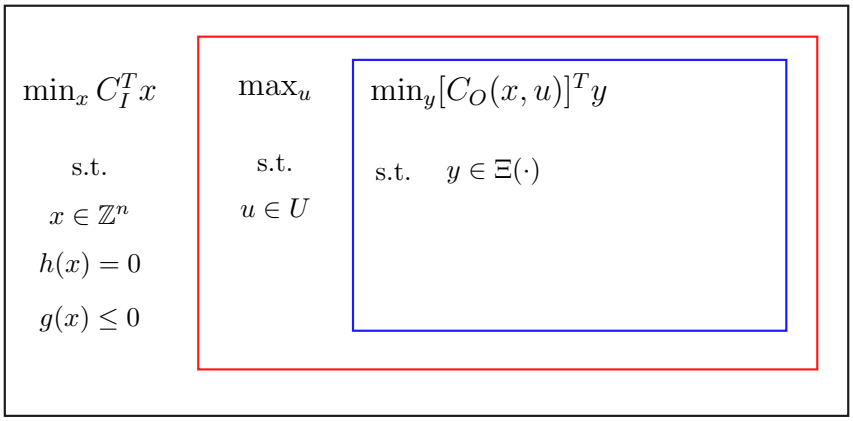

Figure 2: Schematic representation of ARO model formulation; Source: Authors' illustration based on Baringo et al. (2020); Mínguez and García-Bertrand (2016).

2. The second level represents the worst-case uncertainty realization (in the sense of cost maximization) within an uncertainty set (i.e., variables in vector u).
3. The third level represents the corrective actions made to mitigate the effect of the uncertainty realization (i.e., variables in vector y with the vector including operating costs C_O).

Thus, the problem illustrated in Figure 2 involves both a preventive and a curative component. Hence, in many respects, it mirrors the nature of infrastructure planning processes (i.e., project planning subject to uncertainty realizations, for which subsequent mitigation measures are deployed) (Ruiz and Conejo, 2015). In the problem, Ξ and U are the feasibility and uncertainty sets, respectively. Set Ξ identifies the feasible space of the third-level optimization variables, as explained in section 3.1.1, while uncertainty set U is described in section 3.1.2.

3.1.1. Definition of feasibility sets

Set Ξ models the feasible space of third-level optimization variables given the first- and second-level decisions:

$$\begin{aligned} \Xi(x,u) = \{y : \\ A(x,u)\cdot y = b(x,u) : \lambda \\ D(x,u)\cdot y \geq e(x,u) : \mu \\ \} \end{aligned} \tag{1}$$

where A, b, D, and e are matrices with constant parameters depending on the problem configuration, and λ and μ are the dual variable vectors associated with inequality and equality sets of constraints, respectively. Note that the feasibility set Ξ is parameterized in terms of first- and second-level decision variables.

3.1.2. Definition of uncertainty sets

This paper employs a specific type of polyhedral uncertainty sets. Bertsimas et al. (2013b) were among the first to apply such uncertainty sets for the energy network transmission expansion problem. The applicability of polyhedral uncertainty sets to modern energy research paired with the challenges of energy transitions facilitated intensive research and elaborated descriptions of the uncertainty in the literature.

In particular, cardinality-constrained uncertainty sets are advantageous, as they enable the description of uncertainty in the energy markets alongside the improved convergence characteristics of the ARO problems. In such a formulation, the worst-case uncertainty realization corresponds to the vertex of the polyhedron representing the uncertainty set. Thus, polyhedral uncertainty sets can be equivalently characterized by solely modeling the finite set of extremes or vertexes of the polyhedron. This approach has been employed by many researchers (e.g., (Baringo et al., 2019, 2020; Cobos et al., 2018; Mínguez and García-Bertrand, 2016; Zhao et al., 2013)), with binary variables being used to model the extreme-based equivalent for the original cardinality-constrained uncertainty set.

The problem in Figure 2 includes the second-stage decision variable u, which takes values within the known confidence bounds:

$$u \in [\widetilde{u} - \widehat{u}, \widetilde{u} + \widehat{u}] \tag{2}$$

where $\widetilde{u}$ and $\widehat{u}$ represent the vectors of the forecast and fluctuation levels of the uncertain variables, respectively. The corresponding cardinality-constrained uncertainty set, as defined in Baringo et al. (2020), assumes the following form:

$$U = \Big\{ u = \widetilde{u} + diag(z^+)\widehat{u} - diag(z^-)\widehat{u}, \tag{3a}$$

$$z^+, z^- \in \{0,1\}^m, \tag{3b}$$

$$\sum_{k=1}^{m}(z_k^+ + z_k^-) \leq \Gamma, \tag{3c}$$

$$z_k^+ + z_k^- \leq 1, \quad \forall k \Big\} \tag{3d}$$

Eq. (3a) defines the value of the uncertain variable u based on the forecast and fluctuation levels. Eq. (3b) defines the vectors of binary variables z^+ and z^-. Eq. (3c) defines the uncertainty budget Γ, which enables us to control the robustness of the solution. $\Gamma = 0$ implies that all instances of the uncertain variable u are equal to their forecast values (i.e., uncertainty is disregarded). Any positive value of Γ implies that the variable u can deviate from its forecasted value. m indicates the size of the vector of variable u. Eq. (3d) ensures that the uncertain variables in vector u cannot simultaneously be at both their upper and lower bounds.

3.2. Solution procedure

The three-level optimization expressed in Figure 2 is solved via a decomposition technique. Here we again follow past research in the field of RO for power systems. Specifically, we rely on the research of Baringo et al. (2020); Mínguez and García-Bertrand (2016), who employ an efficient coupling method for second- and third-level problems, as well as that of Bertsimas et al. (2013a); Conejo et al. (2016); Mínguez and García-Bertrand (2016), who develop, benchmark, and illustrate a column-and-constraint generation (CCG) algorithm, which is efficient for ARO problems.

The CCG algorithm involves iterative solutions for the master problem and subproblem through the exchange of information provided by the primal decision variables.[1] Finite convergence to the optimal solution is guaranteed given the convexity of the problem (Bertsimas et al., 2013a; Zeng and Zhao, 2013). The algorithm consists of the following three major steps:

1. First, the master problem is solved. The master problem is mainly based on the first-level problem in Figure 2. The master problem uses the solution from the subproblem as input data (i.e., uncertainty realization variables in vector u).
2. Second, the subproblem comprising the second- and third-level problems is solved. The subproblem incorporates input data from the master problem (i.e., the infrastructure expansion decisions in binary vector x).
3. Third, the master problem and the subproblem are iteratively solved until they reach convergence to the optimal solution (i.e., a convergence tolerance is fulfilled).

The following sections provide detailed explanations of the master problem, the subproblem, and the solution procedure.

[1] For this reason, the algorithm is sometimes referred to as "primal Benders' decomposition".

3.2.1. Master problem

The master problem, in a compact form at iteration ν, is as follows:

$$\min_{x,\eta,y^{(\nu)}} Z^M = C_I^T x + \eta \tag{4a}$$

subject to

$$h(x) = 0 \tag{4b}$$

$$g(x) \leq 0 \tag{4c}$$

$$\eta \geq [C_O(x, u^{(\nu')}]^T \cdot y^{(\nu')} \qquad \forall \nu' \leq \nu \tag{4d}$$

$$A(x, u^{(\nu')}) \cdot y^{(\nu')} = b(x, u^{(\nu')}) \qquad \forall \nu' \leq \nu \tag{4e}$$

$$D(x, u^{(\nu')}) \cdot y^{(\nu')} \geq e(x, u^{(\nu')}) \qquad \forall \nu' \leq \nu \tag{4f}$$

where variables in set $\Phi^M = [x, \eta, y^{(\nu')}, \quad \forall \nu' \leq \nu]$ are the optimization variables of the master problem (4).

Overall, the master problem (4) is a relaxed version of the three-level problem in Figure 2, in which the auxiliary variable η iteratively approximates the worst-case value of the second-level objective function. Note that Eqs. (4d)–(4f) are formulated for all realizations of $u^{(\nu')}$, which refers to the optimal values of variables u obtained in the subproblem at iteration (ν'). This procedure is the basis for the term "column-and-constraint generation".

3.2.2. Subproblem

The subproblem is formulated in two steps.

In the first step, we follow the approach used by Baringo et al. (2020); Mínguez and García-Bertrand (2016) to couple the second- and third-level problems depicted in Figure 2. We do this by taking the third-level problem:

$$\min_{y} [C_O(x^{(\nu)}, u]^T y \tag{5a}$$

subject to

$$A(x^{(\nu)}, u) \cdot y = b(x^{(\nu)}, u) : \lambda \tag{5b}$$

$$D(x^{(\nu)}, u) \cdot y \geq e(x^{(\nu)}, u) : \mu \tag{5c}$$

and deriving the corresponding dual problem:

$$\max_{\lambda,\mu} [b(x^{(\nu)}, u)]^T \lambda + [e(x^{(\nu)}, u)]^T \mu \tag{6a}$$

subject to

$$[A(x^{(\nu)}, u)]^T \lambda + [D(x^{(\nu)}, u)]^T \mu = C_O(x^{(\nu)}, u) \tag{6b}$$

$$\lambda : free, \mu \geq 0 \tag{6c}$$

In the second step, we rely on the strong duality equality, which allows us to merge the dual form of the third-level problem (6) with the second-level problem. As a result, the subproblem is formulated as a single-level optimization problem:

$$\max_{u,\lambda,\mu} Z^S = [b(x^{(\nu)}, u)]^T \lambda + [e(x^{(\nu)}, u)]^T \mu \tag{7a}$$

subject to

$$[A(x^{(\nu)}, u)]^T \lambda + [D(x^{(\nu)}, u)]^T \mu = C_O(x^{(\nu)}, u) \tag{7b}$$

$$\lambda : free, \mu \geq 0, u \in U \tag{7c}$$

where variables in set $\Phi^S = [u, \lambda, \mu]$ are the optimization variables of the subproblem (7). Note that at each iteration of ν, the master problem (4) provides the expansion decision x, which is fixed in the subproblem: $x = x^{(\nu)}$. In turn, the subproblem determines the worst-case uncertainty realizations in variable vector u, which are passed to the next iteration of the master problem. Thus, the size of the master problem increases alongside the number of iterations, as a new instance of uncertainty realization is added to the master problem constraints in each iteration.

At this stage, there is only one detail left unfulfilled in formulating the subproblem. The bilinear term $[b(x^{(\nu)}, u)]^T \lambda$ included in the objective function (7a) must be linearized. We follow the example of Mínguez and García-Bertrand (2016) by replacing the bilinear term with the mathematically exact reformulation, which is provided in Section A.8 of Appendix A.

3.2.3. Algorithm

At this point, the master problem (4) and the subproblem (7) have been defined. The problems are iteratively solved via the exchange of information provided by the primal decision variables. The CCG algorithm functions as follows:

1. **Input:** Select the uncertainty budgets Γ^G and Γ^D, and the convergence tolerance ε. These data are selected by the decision-maker.
2. **Initialization:** Initialize the iteration counter ($\nu = 0$) and set the lower bound (LB) and the upper bound (UB) to $-\infty$ and $+\infty$, respectively.
3. Solve the master problem (4).
4. Update the lower bound: $LB = Z^{M*}$.
5. The solution to the master problem contains decision variable vector x^*; set $x^{(\nu)} = x^*$.
6. Solve the subproblem (7).
7. Update the upper bound: $UB = \min\{UB, C^T x + Z^{S^*}\}$, where S^* is the optimal value of the subproblem objective function.
8. If $UB - LB < \varepsilon$, the algorithm stops. The optimal decision is x^*. Otherwise, go to Step 9.
9. Update the iteration counter as follows: $(\nu = \nu + 1)$.
10. Set $u^{(\nu)} = u^*$, where u^* is the optimal decision variable vector of the subproblem obtained in Step 6.
11. Go to Step 3.

Figure 3 presents a visual depiction of the algorithm:

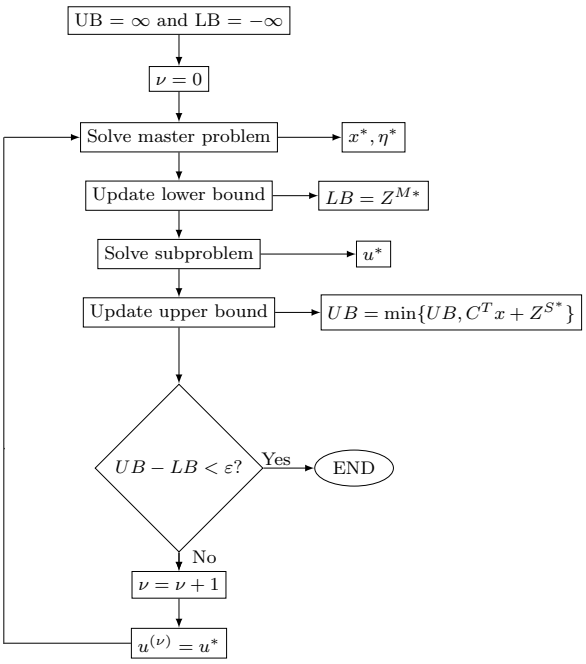

Figure 3: Schematic representation of column-and-constraint generation algorithm. Source: Authors' illustration based on Conejo et al. (2016).

3.3. Empirical application: European gas infrastructure expansion problem

In this section, we apply the ARO method described above to empirically analyze infrastructure expansion needs in the European gas system under unfortunate realizations of demand and supply for 2030.

The resulting model is formulated as a mixed-integer linear problem. The model endogenously determines the worst-case stress for the gas system that falls within the confidence bounds (see section 3.1.2) and iteratively finds the optimal infrastructure expansion plan to address that stress. The objective function aims to minimize the costs of constructing the new infrastructure assets and the operational costs of supplying natural gas under unfortunate realizations of parametric uncertainty subject to the appropriate techno-economic constraints.

The remainder of this section is structured as follows. First, we provide a brief description of the gas network in Subsection 3.3.1. Second, we take a deeper look at the key elements of our analysis: (i) an empirical parametrization of uncertainty budgets in Subsection 3.3.2 and (ii) the set investment options (PCIs) in Subsection 3.3.3. Finally, we discuss the model's other data inputs in Subsection 3.3.4. The formulation of the expansion planning problem for the European gas market is provided in Appendix A.

3.3.1. Gas network

The model structure consists of a network of nodes, each of which represents a country or region. Overall, the gas network (shown in Figure 4) comprises 37 nodes representing the countries and regions that are most relevant in the European gas market. Nodes are connected by gas transmission infrastructure assets, including (i) cross-border pipe-lines within the EU, (ii) cross-border pipelines with non-EU parties (such as the Nord Stream), and (iii) regasification terminals for LNG imports. Overall, the gas network includes 96

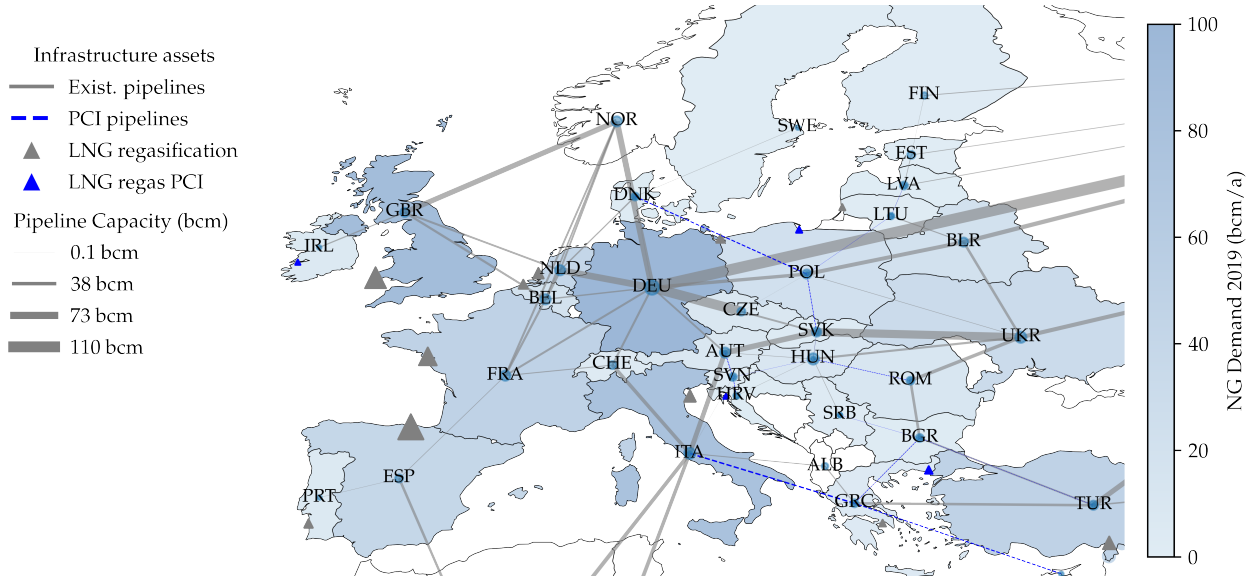

Figure 4: Stylized representation of the European natural gas network. Source: Authors' illustration.

individual pipeline arcs and 11 regasification terminals. Bi-directional pipelines are modeled as two distinct arcs. In our analysis, we model a single representative LNG producer that serves the European market and can ship liquified gas to individual countries based on its total domestic regasification capacity. Regasification terminals included as part of the PCI investment options are similarly modeled as arcs available to be built between the LNG supplier and the destination country. The model neglects friction and pressure drops in the gas network.

3.3.2. Long-term uncertainty characterization: Uncertainty set

Here, in line with Section 3.1.2, we present the parametrization of the uncertainty sets with the data instance relevant for the European gas market. In this paper, we focus on uncertainties surrounding natural gas demand and supply. Both of these sources of uncertainty are characterized by cardinality-constrained uncertainty sets, which are represented mathematically as follows:

$$\Omega = \Big\{ \overline{g}^D_{dt} = \widetilde{G}^D_{dt} + z^D_{dt} \cdot \widehat{G}^D_{dt} \quad \forall d, \forall t \tag{8a}$$

$$\overline{g}^P_p = \widetilde{G}^P_p - z^P_p \cdot \widehat{G}^P_p \quad \forall p \tag{8b}$$

$$\sum_{d \in D, t \in T} z^D_{dt} \leq \Gamma^D \tag{8c}$$

$$\sum_{p \in P} z^P_p \leq \Gamma^P \tag{8d}$$

$$z^D_{dt} \in \{0,1\} \quad \forall d, \forall t \tag{8e}$$

$$z^P_p \in \{0,1\} \quad \forall p \Big\} \tag{8f}$$

Constraints (8a) and (8b) express the uncertain variables—the demand and supply vectors—with respect to projected reference values and their deviations, resulting in system stress. In Eq. (8a), $\overline{g}^D_{dt}$ denotes the uncertain demand in each node and time step, $\widetilde{G}^D_{dt}$ denotes the reference value, and $\widehat{G}^D_{dt}$ denotes the possible

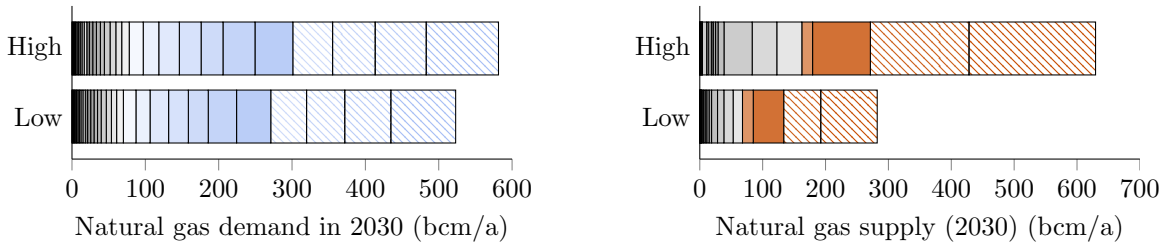

(a) Demand uncertainty set

(b) Supply uncertainty set

Figure 5: Scenario projections used for the construction of the uncertainty sets. Each segment represents the annual demand level (left panel) and supply potential (right panel) of an individual country. Source: ENTSO-G (2020)

.

deviation from the reference value. Eq. (8b) corresponds similarly to the network supply. Note that the unfortunate realization of supply is modeled on an annual basis. Thus, Eq. (8b) does not feature a time step index. This reflects the temporal nature of parametric uncertainty in the model: cold-winter gas demand spikes on the one hand; policy- and technology-driven development of annual gas supply potentials on the other hand. Constraints (8c)–(8f) follow the explanation in Section 3.1.2.

Data-driven approaches to constructing suitable uncertainty sets are the common tools used in ongoing research (Ruiz and Conejo, 2015). Such approaches incorporate available data to devise uncertainty sets that ensure that the random variables under investigation are contained in defined probability distributions. We construct the uncertainty sets for natural gas demand and supply volumes based on scenario projections for 2030, which stem from the scenario framework adopted in the Ten-Year Network Development Plan (ENTSO-G, 2020).[2] The reference values adopted for the uncertainty sets correspond to the optimistic scenario projections regarding supply security (i.e., mild winter demand levels and the highest available supply volumes). The uncertainty sets enable the investigation of unfortunate realizations with respect to 2030 supply security. The demand and supply volumes covered by the cumulative budgets are displayed in Figure 5. The bar graphs comprise the scenario-specific demand and supply projections for the individual countries and/or suppliers in the model.

In line with the analysis of the PCIs' contributions to supply security, the demand uncertainty budgets are constructed to reflect the realization of a cold-winter peak demand event across Europe. The demand budgets considered are allocated across five winter months (November–March). Deviations per month incorporated are based on historical peaks of gas demand in each modeled country over the last decade (Eurostat, 2020). To provide a more explicit illustration of how the uncertainty budgets are employed in the model, Figure B.11 in Appendix B illustrates the worst-case demand realizations given the uncertainty budget of $\Gamma^D = 10$. The demand spikes materialize in a way that represents the worst-case scenario in terms of the gas system operational costs.

Regarding the employed supply uncertainty budget, the deviations represent the difference in the projected 2030 supply potentials between the most optimistic and the most pessimistic supply scenarios. In contrast to the demand uncertainty budgets, the supply uncertainty budgets are constructed on an annual basis (i.e., an endogenously determined supply cut applies to the entire year). As detailed above, the supply

[2]Projections are sourced from the National Trends and Global Ambition scenario.

cost curves for the six largest gas producers[3] are modeled in a piece-wise fashion, resulting in a merit order-style supply stack. Each individual supply stack consists of five individual segments. For EU producers, we assume a simplified per-unit cost. As illustrated in Figure B.11 in Appendix B, the endogenous realization of a supply drop given the uncertainty budget of $\Gamma^S = 10$ entails cutting supply from the five supply fields, which results in the worst-case scenario (i.e., the highest possible increase in the system's operational costs).

3.3.3. Investment options: Projects of Common Interest

As indicated above, our analysis focuses on the economic viability of proposed gas infrastructure projects awarded the status of PCI. To qualify as PCIs, projects must demonstrate significant improvement in market integration in at least two EU countries, enhance competition in energy markets, and contribute to the energy security (European Commission, 2021a). PCIs are eligible to receive public funding from the Connecting Europe Facility, which can cover up to 50% of project-specific investments. The most recent PCI list—the fourth such list, approved at the beginning of 2020—includes 32 gas-related infrastructure projects, most of which focus on enhancing regional infrastructure in Central and Southeastern Europe. According to European Commission (2020), the completion of these 32 projects will facilitate a well-interconnected and shock-resilient gas network, providing all EU member states with access to at least three gas supply sources or the global LNG market.

In this analysis, we focus on the cross-border pipelines and regasification projects from the fourth PCI list. The individual projects are incorporated as discrete investment decisions (i.e., they constitute separate connections between the countries under consideration). Thus, the projects spanning multiple countries are split up into their constituent cross-border connections. The investment options comprise 26 pipeline arcs (13 bi-directional cross-border pipeline connections) and four LNG regasification terminals. Data on project-specific investments and the associated capacities of the considered PCIs was obtained from various publicly available sources (ACER, 2019; Oil Change International, 2019; Three Seas Iniative, 2019; European Union, 2020; Global Energy Monitor, 2021).

The projects included in the analysis are illustrated in Figure 6. A table with information relevant to the individual pipeline and regasification terminal projects can be found in Appendix C.

3.3.4. Other input data

Network data for the model (i.e., existing cross-border pipelines and regasification terminals in Europe) is primarily sourced from the ENTSOG (2020). For the purposes of this analysis, we assume that the Nord Stream 2 project is completed and at full operational capacity in 2030 and that the terms of the recently negotiated Russia-Ukraine transit deal, in which there is a set minimum capacity obligation of 40 bcm/year through 2024, are extended. The analysis assumes that gas flows from Russia via Ukraine are restricted to this minimum volume (Pirani and Sharples, 2020).

Transmission costs are calculated using linear functions of pipeline length, pipeline type (on-shore/offshore), and transmission cost factor per unit of gas volume and unit of distance. The transmission cost factor is based on the natural gas modeling literature (Chyong and Hobbs, 2014; Egging and Holz, 2019). The production costs of the largest suppliers are modeled based on a piece-wise approximation of the Golombek logarithmic cost function, which stems from (Egging and Holz, 2019) and (Riepin and Müsgens, 2022).

[3]Russia, Norway, LNG, Caspian region, Algeria, Ukraine

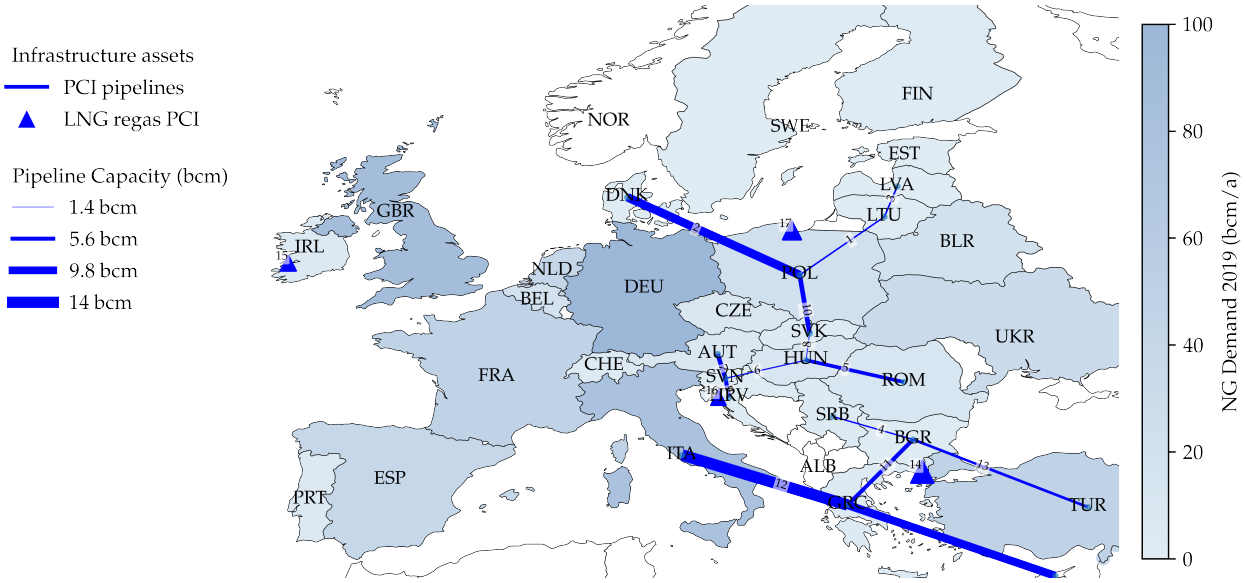

Figure 6: Stylized representation of the European natural gas network. Source: Authors' illustration.

For smaller domestic producers, we assume a constant per-unit production cost. Similarly, we model the representative LNG supply cost curve in a piece-wise linear manner to reflect the LNG supply structure for Europe. The constructed LNG cost curves include liquefaction and regasification costs. LNG shipping costs are calculated as a capacity-weighted function of distance between nodes. The supply cost curves for Europe in 2030 are calibrated based on BEIS (2016).

Data concerning country-specific storage capacities as well as maximum monthly injection and withdrawal rates are sourced from the GIE transparency platform. The data are aggregated at the national level (i.e., each country has one representative storage node). Since the optimization problem focuses on a single year, storage levels at the beginning and end of the year are fixed. We do not explicitly consider the demand-side response in our analysis, as data on country-specific potentials are generally unavailable, and the role of demand-side response as a flexibility tool in the European gas market is limited (European Commission, 2015). Thus, we incorporate an option for gas demand shedding at a penalty cost.

4. Results and discussion

The results section is organized as follows. Section 4.1 focuses on the robust expansion plan of European gas infrastructure considering the PCIs and the worst-case realizations of cold-winter demand spikes under increasing uncertainty budgets. Afterward, Section 4.2 expands this analysis by assuming that the solution space is not limited to the set of PCIs and including the option to expand all existing arcs in the EU. Section 4.3 evaluates the realization of PCI investments when incorporating uncertainty budgets representing both demand spikes and supply shortages. Finally, Section 4.4 examines the extent to which the composition of robust investments changes when introducing an investment budget.

It should be noted that the analysis and visualization of each scenario entail some modifications to the model solution space (i.e., the set of possible investment options) and uncertainty budgets (Γ_D and Γ_S).

We explain these modifications at the start of each subsection. Neither the ARO model nor the solution algorithm are changed across the considered scenarios.

In all cases, the results are computed in GAMS[4] using CPLEX solver on a computer with an Intel Core i7-8750 CPU at 2.20 GHz and 16 GB of RAM. The ARO model for all of the following scenarios is successfully converged (i.e., $UB - LB = 0$).

4.1. Robust expansion considering cold-winter gas demand spikes

This section investigates how the optimal (in terms of system robustness) investment plan changes with respect to different values of the demand uncertainty budget Γ_D. The analysis is based on the following assumptions:

1. Investment decisions are made from the set of PCIs (see Appendix C).
2. Uncertainty budget Γ_D is fixed to [0, 10, 30, 60]. Note that the worst-case realizations of unknown parameters are determined endogenously by the model algorithm. Empirically, a unit of uncertainty budget for demand entails one month of peak demand in a specific node (see Section 3.3.2 for further details). As this subsection focuses on gas demand uncertainty, supply uncertainty is not considered, meaning Γ_S is fixed to 0 (i.e., available supply is based on the reference scenario).
3. No limits are enforced on investment budget availability (i.e., constraint A.1c in Appendix A is relaxed).

Figure 7 presents the results of this analysis. The choropleth maps illustrate gas demand spikes associated with the worst-case demand realization under the uncertainty budget Γ_D. The realized investments are displayed as lines connecting two countries (pipelines) and triangles (regasification terminals). Note that for each scenario, the projects built represent the optimal expansion plan for the respective uncertainty budget. Above the choropleth maps, summary tables offer a quick comparison of investments across all scenarios.

The bottom row of Figure 7 represents an estimated CAPEX scenario, which assumes that project investors do not receive financial grants from the EU. This scenario can be viewed as an analysis of whether PCIs are beneficial from a societal perspective. The results show that only two projects are built: the HU–Sl pipeline ($\Gamma_D = [0, 10, 30, 60]$) and the PL–SK pipeline ($\Gamma_D = 60$). The HU–Sl pipeline notably appears in the optimal solution under all uncertainty budgets, indicating the high value of this project to the gas system. According to the European Commission, the connection between the gas markets in Sl and HU aims to diversify the gas supply in the region. The pipeline will improve diversification of gas sources (LNG sources from the Adriatic region), which are available in SI and enable access to gas storages in HU for SI users (European Commission, 2021b). The PL–SK pipeline aims to create a north–south gas corridor in Eastern Europe and boost gas supply security throughout the region (Eustream, 2021). The model results suggest that the project provides value to the system amid increased demand uncertainty (scenario $\Gamma_D = 60$ entails demand spikes in Poland).

The top row of Figure 7 represents a subsidized CAPEX scenario, which assumes that, due to their PCI status, the projects receive financial support from the Connecting Europe Facility. This scenario can be viewed as an analysis of whether PCIs are profitable from a business perspective (i.e., whether their value

[4]The General Algebraic Modeling System

exceeds lower, subsidized investment costs). The results are notably different, as the optimal expansion plan includes a minimum of three projects built in $\Gamma_D = 0$ and as many as eight projects under the uncertainty budget $\Gamma_D = 80$. The two projects built across all of the uncertainty budgets are the regasification terminals in Ireland and Croatia. The latter of these two, the KrK LNG terminal in Croatia, is the first LNG project of its kind in the country with an initial capacity of 2.6 bcm/a, which is equivalent to the annual gas demand in Croatia. With increasing uncertainty budget values, seven further projects are realized, resulting in stronger interconnection among the Baltic states (LV–LT), a new physical connection between the Baltic states and Poland (LT–PL), the north–south gas corridor (PL–SK), a regasification terminal in Greece (GR–LNG), greater supply diversification in the Balkan region (BG–SB, GR–BG, HR–SL), and increased access to LNG through terminals in Greece and Croatia.

One interesting observation in the subsidized CAPEX scenario is that the optimal expansion plan captures all of the PCIs that are in the final realization stage. It should be noted that the LNG terminal in Croatia is operational starting January 2021 and four other projects that are currently under construction (LT–PL, BG–SB, PL–SK, GR–BG) have received significant financial support through grants and low-interest loans (see Appendix C). The results of the ARO model suggest that real-world construction efforts have been targeted toward the most promising projects from a systems perspective. These projects appear to be well-situated to ensure supply security amid increasing demand uncertainty. Nevertheless, from a societal perspective (i.e., absent of subsidies), the results indicate that the vast majority of PCIs are not economically viable under our model assumptions—even when the system is stressed by the ARO algorithm with regard to cold-winter gas demand spikes.

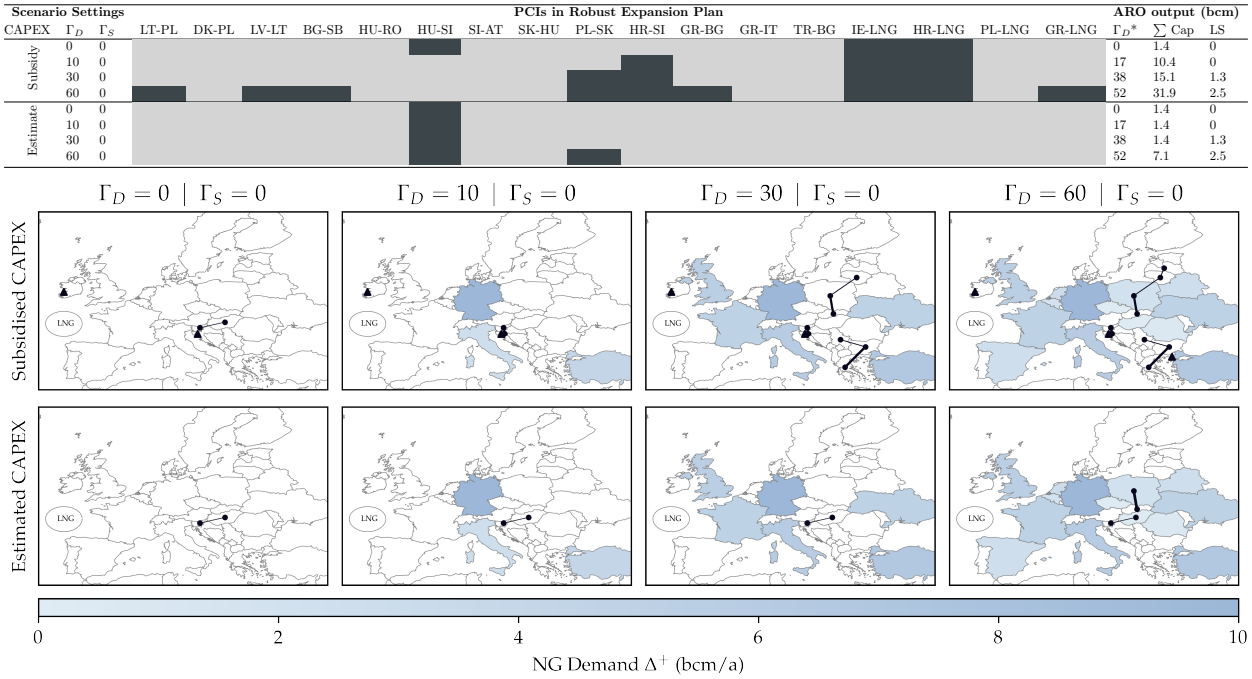

Figure 7: Robust expansion plan considering a set of PCIs under four uncertainty budgets for gas demand (columns). The horizontal axis aggregates demand spike values per country on an annual basis. Scenarios include two CAPEX assumptions (rows).

The results demonstrate a general trend toward an increasing number of investments alongside greater system stress (i.e., an increasing demand uncertainty budget). Additional projects are built to hedge against increasing levels of demand uncertainty, either by connecting countries in which demand spikes materialize to other countries or by interconnecting regions to diversify their supply and alleviate system congestion.

4.2. Robust expansion considering cold-winter gas demand spikes and investment options beyond the PCI list

The expansion options considered in the above section were discrete expansion options limited to the set of PCIs. This section evaluates whether the expansion of other existing infrastructure assets would be preferable from a systems perspective to hedge against the worst-case realization of demand across Europe. The analysis incorporates the following assumptions:

1. Investment decisions are made from the union of two sets: (i) PCIs and (ii) 20% capacity increase on any arc in the gas infrastructure network (pipelines or regasification terminals) located in the EU.[5]
2. Uncertainty budgets are fixed identically to 4.1: $\Gamma_D = [0, 10, 30, 60]$, $\Gamma_S = 0$.
3. No limits are enforced on investment budget availability (i.e., constraint A.1c in Appendix A is relaxed).

Figure 8 illustrates the results. The choropleth maps follow the example of the previous section, illustrating the gas demand realizations and the respective investments under a range of uncertainty budgets.

One notable observation from the subsidized CAPEX scenario (top row of Figure 8) is that, despite expanding the investment options to more than 100 projects (17 PCIs and 92 non-PCI projects), the solution of the ARO model comprises nine projects—the majority of which are PCIs. Hence, our modeling exercise confirms the estimates of national TSOs on gas flows under the system stress and the promising projects from to address that stress. This result suggests that, despite the high degree of interconnectivity in the European gas network, certain PCIs are promising from a business perspective (i.e., in a presence of subsidy) in the face of the worst-case demand realization.

The new non-PCI projects that are realized as a part of the optimal expansion plan include one pipeline (UA–PL) and two regasification terminals in Belgium and France.

Interestingly, even though the UA–PL pipeline is not listed on the PCI list, the interconnector is highly likely to assume operations by the end of 2022, as the Ukrainian and Polish TSOs signed an agreement in 2016 to advance the construction of the project (Energy Community, 2021). The project was conferred a code in the ENTSOG TYNDP 2020[6]. Although a relatively small addition in terms of transmission capacity, expansion of the pipeline would facilitate the further integration of Ukrainian storage facilities into the European gas system. The project is solely realized under a relatively large uncertainty budget of $\Gamma_D = 60$, which indicates the potential flexibility that it would provide the system amid widespread cold-winter demand peaks.[7]

[5] The capacity of new investment options—a total of 92 arcs—is parametrized to a 20% increase in existing infrastructure items; the average capacity is comparable to the average size of the PCI projects. The CAPEX of the new investment options is parametrized based on the 75th percentile of the PCIs' investment per bcm of capacity. The factors per bcm applied are computed separately for pipelines and LNG projects.

[6] In the TYNDP 2020, the project is listed under the code "TRA-A-621" for the Polish section and the code "TRA-A-561" for the Ukrainian section (ENTSOG, 2020)

[7] The integration of Ukrainian storage facilities into the European gas system brings further benefits not explicitly captured by our model (e.g., allowing vast Ukrainian storage capacity to be used by Polish companies that face strategic storage obligations).

Another observation that stands out in Figure 8 is the partial substitution of PCIs by non-PCI projects. In particular, the two new LNG terminals reroute LNG flows to Central Eu-rope, compromising the economic viability of the LNG terminal in Greece and the two PCI pipe-lines previously built to bring gas north from the Adriatic region (the GR–BG and BG–SB pipe-lines are not built in this scenario). This result can be understood in the context of the system-wide optimization that the model entails.

The results are markedly different in the estimated CAPEX scenario (bottom row of Figure 8). As with the results in Section 4.1, the HU–Sl pipeline appears in the optimal solution under all uncertainty budgets. However, the other two projects built under high uncertainty budgets (UA–PL and FR–LNG) are not from the PCI set. It is unsurprising to see the UA–PL pipeline appearing in the model solution in this scenario, as, in reality, the project is also completed without the subsidy. Overall, these results reflect the importance of efficient trade and storage utilization in a system as complex as the European gas market.

The results of this section provide further insight into robust gas infrastructure expansion under uncertainty budgets. The insights (i) confirm that, without financial support, most of the PCIs are unlikely to be realized; (ii) point toward the system benefits of the HU–Sl and UA–PL pipelines; and (iii) indicate that, in a subsidized setting, PCIs provide more system value in guarding against demand uncertainty than the infrastructure expansion options beyond the PCI list; this finding aligns with the strategic aims of the project list. The observation made in Section 4.1 that the ARO solution entails more investments under higher Γ_D values holds for this case as well.

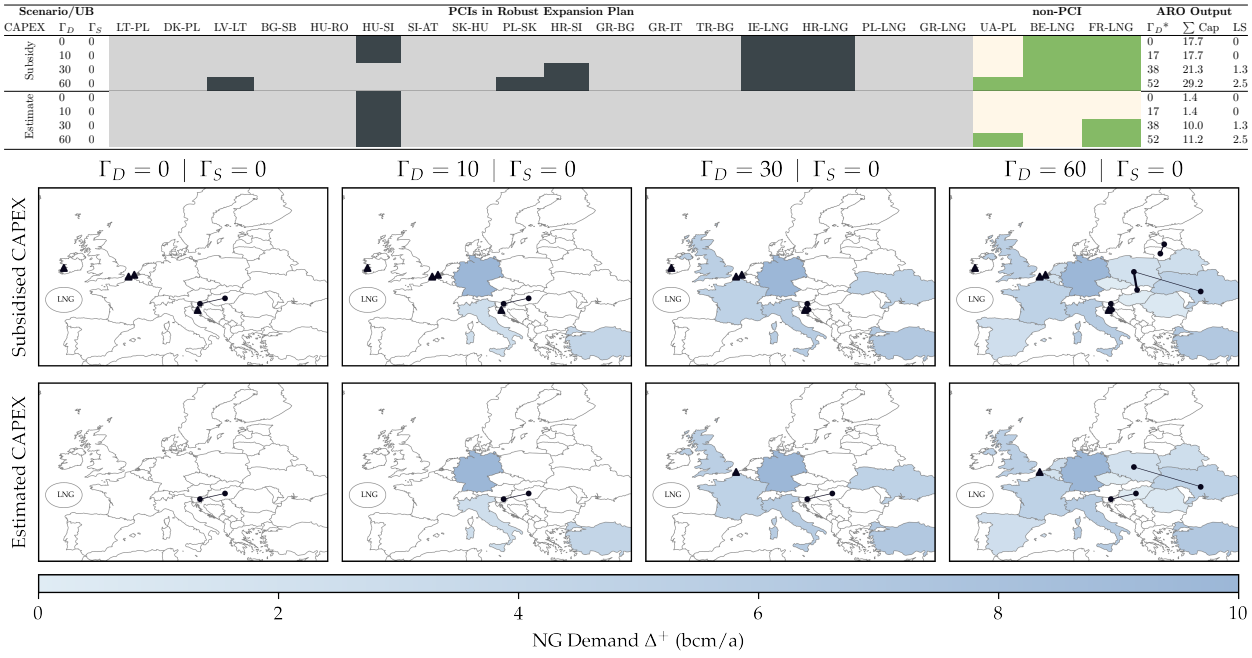

Figure 8: Robust expansion plan considering a set of PCIs and a 20% capacity increase option for any arc in the network (pipeline or regasification terminal) located in the EU. Scenarios include four uncertainty budgets for gas demand (columns) and two CAPEX assumptions (rows). The horizontal axis aggregates demand spike values per country on an annual basis.

4.3. Robust expansion considering cold-winter demand spikes and supply shortages

Moving beyond an isolated analysis of 2030 demand uncertainty, this section investigates the optimal robust expansion plan considering the worst-case realizations of both gas demand and supply within the uncertainty budgets. The analysis is based on the following assumptions:

1. Investment decisions are made from the set of PCI projects.
2. Uncertainty budgets are fixed as follows: $\Gamma_D = [0, 10, 30, 60]$, $\Gamma_S = [1, 2]$.[8] Empirically, a unit of the uncertainty budget entails a shortage in one production field in a specific node over the entire modeled year (see Section 3.3.2 for further details).
3. Investment costs are based on the subsidized CAPEX scenario.
4. No limits are enforced on investment budget availability (i.e., constraint A.1c in Appendix A is relaxed).

The results of this analysis are reported in Figure 9. The choropleth maps now illustrate the worst-case realizations of both demand and supply under the uncertainty budgets. As with the results in the previous sections, the Γ_D steps are visualized as columns, while the Γ_S steps form two rows for each CAPEX scenario.

Figure 9 demonstrates several interesting features of the robust solution.

First, the supply uncertainty budget of $\Gamma_S = 1$ eliminates some projects from the solution space. These include pipelines in the Baltic states and Central Europe (LT–PL, LV–LT, PL–SK). The projects aimed at facilitating supply diversification in the Balkan region as well as two regasification terminals in Ireland and Croatia remain a part of the optimal expansion plan. Furthermore, this scenario includes (i) one additional investment (LNG terminal in Greece), which brings greater regasification capacity to the Adriatic region, and (ii) the construction of the GR–BG pipeline, which supports the GR–LNG terminal. As the resulting worst-case supply realization under $\Gamma_S = [1]$ constitutes a supply drop of ca. 50 bcm/a from Russia, this solution is aimed at a cost-optimal substitution of the missing supply.

Second, the supply uncertainty budget of $\Gamma_S = 2$ yields a situation in which an additional 45 bcm/a of LNG supply is unavailable. This further decreases the number of realized projects. As expected, new regasification projects are not viable in this scenario due to a shortage of available LNG supply. This has a reverberating effect, as the projects aimed at bringing gas north by connecting the Adriatic region with Central Europe (GR–BG, HR–Sl, BG–SB) do not appear in the robust solution. The sole realized project is the HU–SL interconnector. This can be explained by its central location and the importance of access to gas storage in Hungary for consumers in Slovenia and neighboring countries.

Third, the results of this section highlight the general trend of investment dynamics when supply drops are incorporated into the uncertainty budget—the ARO solution generally entails fewer investments. This outcome stems from the fact that investment decisions associated with the robust solution under supply uncertainty entail interplay between capital costs, load-shedding costs, and network topology. The results demonstrate that additional LNG projects may be viable to hedge against pipeline supply shortages (e.g., GR–LNG, supply drops in Russia); however, if the supply of both Russian pipeline gas and LNG fall into the uncertainty budget, the economic viability of projects is compromised due to the system's overall supply shortage. This is indicated by load-shedding volumes of ca. 65 bcm/a.

[8] A model run with $\Gamma_S = [0]$ is discussed in Section 4.1.

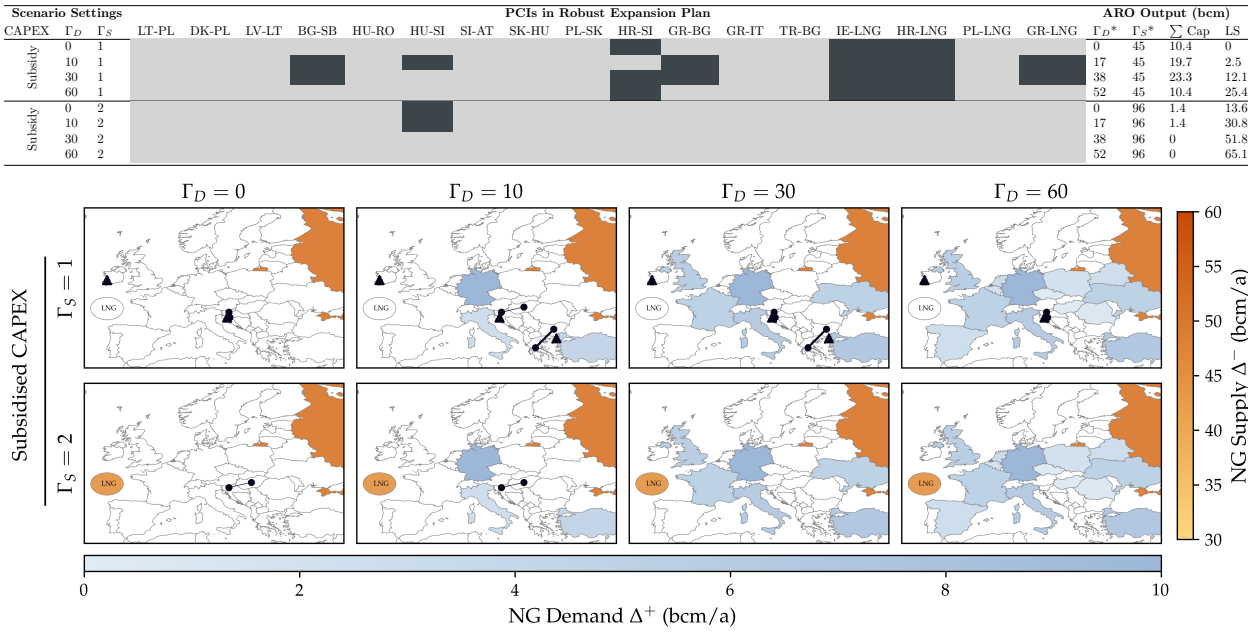

Figure 9: Robust expansion plan considering a set of PCIs under different uncertainty budgets for gas demand (columns) and supply (rows). Horizontal axis aggregates demand spike values on an annual basis per country. Vertical axis presents annual supply cut per country.

4.4. Robust expansion considering an investment budget

This section evaluates how budget availability can influence the composition of investment decisions in the robust solution. The analysis is conducted with the following assumptions:

1. Investment decisions are made from the set of PCI projects.
2. Uncertainty budgets are fixed as follows: $\Gamma_D = 60$, $\Gamma_S = 0$.
3. Investment costs are based on the subsidized CAPEX scenario.
4. An annualized investment budget has an upper limit that takes values of 20, 40, and 60 MEUR (i.e., constraint A.1c in Appendix A is binding).

The robust solution considering assumptions 1 and 2 and neglecting a budget constraint is detailed in Section 4.1. The model configuration yields the results reported in Figure 7 (row with $\Gamma_D = 60$). The composition of investments obtained in the model configuration entails an annualized investment of 62.8 MEUR. Using this value as a reference, we construct a set of sensitivity cases in which the annualized investment budget is assumed to be 20, 40, and 60 MEUR.

Figure 10 illustrates the optimal investments for each budget scenario. Note the new columns with solution information relevant to this section. IB* reports the cost of an annualized investment budget in MEUR per scenario. Each value is less than the budget limit set by the constraint due to the discrete nature of the investment decisions. ΔIC reports the difference between the most expensive investment mix (with no constraint imposed on IB) and the optimal solution in each scenario. ΔTC reports the difference between the total cost (objective value of the subproblem) of each scenario and the total cost of the solution absent the investment budget. The optimization framework of the ARO model ensures that (a) $\Delta TC \geq \Delta IC$ (i.e.,

investment decisions must have a positive (or no) impact on the objective value and that (b) the model setup void of an investment budget yields, by definition, the lowest objective value.

In the absence of an investment budget (the reference case, row IB = inf in Figure 10), the ARO model prefers nine PCIs, among them three regasification terminals and six pipelines. When adding a budget restriction, the ARO model reduces the number of investments to avoid violating the budget.

With a budget of 20 MEUR, four projects are realized: LT–PL to establish a physical connection between the Baltic states and Poland; LV–LT to strengthen interconnection among the Baltic states; and HR–LNG and HR–Sl to provide the Balkan region with access to LNG. This result aligns well with the current project status of the PCIs, as the four projects built in the robust solution are either already operational or in the final stage of development. With a budget of 40 MEUR, a regasification terminal in Ireland is added to the investment mix. Increasing the budget to 60 MEUR adds a regasification terminal in Greece as well as two pipeline projects, GR–BG and BG–SB, which connect the Greek regasification terminal to the Balkan region. Eliminating the budget yields a single additional project—the PL–SK pipeline.

Figure 10 depicts how decreasing the investment budget results in a gradual increase in total costs. The behavior takes place due to an incremental increase in the operational costs. Under the model optimization framework, the investment decision is based on the equality of the investment costs and the benefits (i.e., a decrease in operational costs) of using the new infrastructure item. For this reason, no other PCI is realized despite the unlimited investment budget—an increase in the annual investment payment ΔIC would not compensate for the decrease in the total costs.

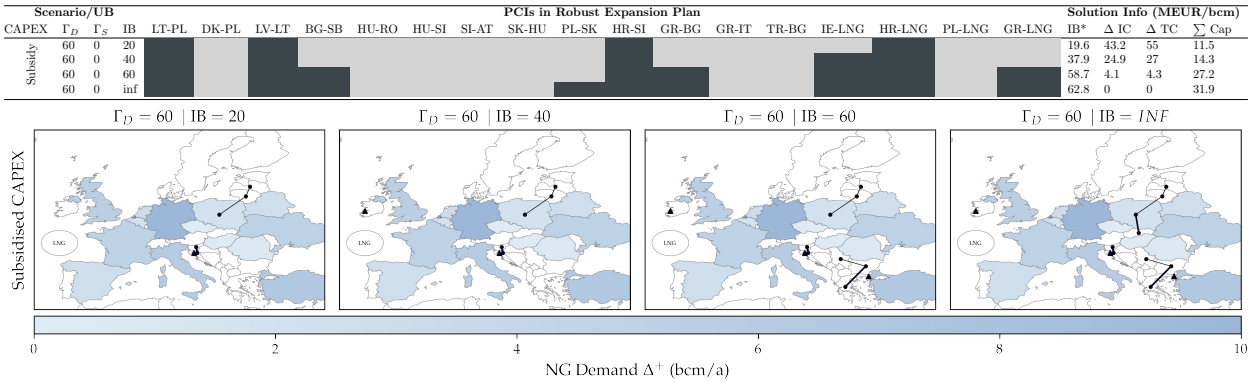

Figure 10: Robust expansion plan considering a set of PCIs subject to investment budgets. Scenarios entail four annualized budgets (columns).

5. Summary and outlook

The European natural gas market is subject to evolving market conditions and energy and climate policy dynamics that intensify uncertainty regarding the long-term projections of both demand and supply. This paper addresses this matter by suggesting an adaptive robust optimization framework for gas infrastructure expansion planning under these uncertainties. In particular, we analyze the value of Projects of Common Interests—gas infrastructure projects supported by EU public funds—in ensuring supply security in 2030. Methodologically, our analysis contributes to the literature by demonstrating the first application of adaptive robust optimization for gas infrastructure expansion planning considering long-term uncertainties.

In terms of demand uncertainty, we draw the conclusion that increasing levels of uncertainty, represented by the increasing value of uncertainty budgets, lead to additional investments. These investments aim to hedge against demand uncertainty, either by interconnecting regions to diversify their supply and alleviate system congestion or by connecting countries in which cold-winter demand spikes materialize to neighboring countries with large storage facilities (e.g., PL-UA pipeline).

There is a clear distinction in the incidence of project realization between scenarios with subsidized CAPEX and scenarios with estimated CAPEX. Without a substantial level of financial support, only a small subset of proposed projects are built. This finding coincides with recent analysis suggesting the superfluous nature of the projects proposed in the fourth Projects of Common Interest list (Artelys, 2020).

The results of the scenario run considering a possibility of expanding the capacity of existing transmission infrastructure assets reveal that that the subsidized investments in the Projects of Common Interest remain predominantly represented in the robust solution. These investments are complemented by the expansion of LNG infrastructure in Northwest Europe and by construction of UA–PL pipeline that enables the use of large Ukrainian storage facilities when hedging against demand spikes in Central Europe. The HU–Sl and UA–PL pipelines are built even in a non-subsidized setting, which highlights the system benefits of these projects. Overall, these results reflect the importance of efficient trade and storage utilization in a system as complex as the European gas market.

An interesting observation is that introducing an investment budget result in the prioritization of a particular set of Projects of Common Interest—those that are either already operational or in the final stage of development. This result suggest that real-world construction efforts have been targeted toward the most promising projects from a systems perspective.

When supply drops are incorporated into the model, the general trend of investment dynamics is that the robust solution entails fewer investments with increasing supply uncertainty budget. This observation stems from the fact that investment decisions entail interplay between capital costs, load-shedding costs, and network topology. Specifically, the robust expansion plan utilizes the group of projects associated with facilitating access to Adriatic LNG supplies to hedge against supply drop from Russia. However, increasing the value of the uncertainty budget further, both Russian pipeline gas and LNG fall into the uncertainty budget. In this case, the economic viability of LNG projects is compromised due to the system overall supply shortage.

Our analysis contributes to the extant research on modeling uncertainty in the European gas market. In terms of methodology, our work can serve as the foundation for future research aimed at quantifying the value of gas infrastructure projects. However, our analysis must be considered in the proper context. Due to the scope of our analysis and the complexity of adaptive robust optimization, the employed linear model fails to incorporate demand elasticity and neglects strategic behaviors in gas markets. Furthermore, the aggregated nature of the transport model abstracts from physical gas flows and the associated non-linearities. The model application also entails certain simplifications (e.g., designating a central European LNG supplier instead of explicitly modeling LNG liquefaction and regasification terminals).

Several questions remain for further research. In particular, demand uncertainty sets can be configured to incorporate regional correlation regarding cold-winter peaks. In our analysis, the worst-case demand realizations were assessed at the system level. Given that the impacts of extreme cold are likely to manifest regionally, uncertainty sets can be formulated to reflect spatial correlations. Future investigations could

focus on storage assets from the Projects of Common Interests list, which were not within the scope of our analysis. Furthermore, it would be interesting to see research that, while inspired by our methodology, focuses on the markets for other products (e.g., hydrogen).

References

Abada, I., Jouvet, P.A., 2012. A stochastic generalized Nash-Cournot model for the northwestern European natural gas markets: The S-GaMMES model. URL: https://ideas.repec.org/p/cec/wpaper/1308.html.

Abada, I., Massol, O., 2011. Security of supply and retail competition in the European gas market. Energy Policy 39, 4077–4088. URL: http://www.sciencedirect.com/science/article/pii/S0301421511002230, doi:10.1016/j.enpol.2011.03.043.

Abrell, J., Chavaz, L., Weigt, H., 2019. Dealing with Supply Disruptions on the European Natural Gas Market: Infrastructure Investments or Coordinated Policies? 1155002547. doi:10.2139/ssrn.3425739.

ACER, 2019. Consolidated Report on the Progress of Electricity and Gas Projects of Common Interest - 2019. Technical Report. Agency for the Cooperation of Energy Regulators. Ljubljana.

Artelys, 2020. An updated analysis on gas supply security in the EU energy transition. Technical Report. Artelys Optimization Solutions. Paris.

Aßmann, D., Liers, F., Stingl, M., 2019. Decomposable robust two-stage optimization: An application to gas network operations under uncertainty. Networks 74, 40–61. doi:10.1002/net.21871.

Aven, T., 2013. On the meaning of a black swan in a risk context. Safety Science 57, 44–51. URL: http://dx.doi.org/10.1016/j.ssci.2013.01.016, doi:10.1016/j.ssci.2013.01.016.

Baltensperger, T., Füchslin, R.M., Krütli, P., Lygeros, J., 2017. European Union gas market development. Energy Economics 66, 466–479. URL: https://www-sciencedirect-com.lib-e2.lib.ttu.edu/science/article/pii/S0140988317302396{#}f0005, doi:10.1016/J.ENECO.2017.07.002.

Baringo, A., Baringo, L., Arroyo, J.M., 2019. Day-ahead self-scheduling of a virtual power plant in energy and reserve electricity markets under uncertainty. IEEE Transactions on Power Systems 34, 1881–1894. doi:10.1109/TPWRS.2018.2883753.

Baringo, L., Baringo, A., 2018. A stochastic adaptive robust optimization approach for the generation and transmission expansion planning. IEEE Transactions on Power Systems 33, 792–802. doi:10.1109/TPWRS.2017.2713486.

Baringo, L., Boffino, L., Oggioni, G., 2020. Robust expansion planning of a distribution system with electric vehicles, storage and renewable units. Applied Energy 265, 114679. URL: https://doi.org/10.1016/j.apenergy.2020.114679, doi:10.1016/j.apenergy.2020.114679.

BEIS, 2016. Fossil Fuel Supply Curves. Technical Report. UK Department for Business, Energy & Industrial Strategy. London. URL: www.nationalarchives.gov.uk/doc/open-government-.

Bertsimas, D., Brown, D.B., Caramanis, C., 2011. Theory and applications of robust optimization. SIAM Review 53, 464–501. doi:10.1137/080734510, arXiv:1010.5445.

Bertsimas, D., Litvinov, E., Sun, X.A., Zhao, J., Zheng, T., 2013a. Adaptive robust optimization for the security constrained unit commitment problem. IEEE Transactions on Power Systems 28, 52–63. doi:10.1109/TPWRS.2012.2205021.

Bertsimas, D., Litvinov, E., Sun, X.A., Zhao, J., Zheng, T., 2013b. Multistage adaptive robust optimization for the unit commitment problem. IEEE Transactions on Power Systems 28, 52–63. doi:10.1109/TPWRS.2012.2205021.

Birge, J.R., Louveaux, F., 2011. Introduction to Stochastic optimization. 1, Springer, New York, NY. doi:10.1007/978-1-4614-0237-4.

Chen, B., 2016. Applications of optimization under uncertainty methods on power system planning problems. Doctoral thesis. Iowa State University. doi:10.1017/CBO9781107415324.004, arXiv:arXiv:1011.1669v3.

Chyong, C.K., Hobbs, B.F., 2014. Strategic Eurasian natural gas market model for energy security and policy analysis.Formulation and application to South Stream. Energy Economics 44, 198–211. URL: http://dx.doi.org/10.1016/j.eneco.2014.04.006, doi:10.1016/j.eneco.2014.04.006.

Cobos, N.G., Arroyo, J.M., Street, A., 2018. Least-cost reserve offer deliverability in day-ahead generation scheduling under wind uncertainty and generation and network outages. IEEE Transactions on Smart Grid 9, 3430–3442. doi:10.1109/TSG.2016.2632622.

Collins, S., Deane, J.P., Poncelet, K., Panos, E., Pietzcker, R.C., Delarue, E., Ó Gallachóir, B.P., 2017. Integrating short term variations of the power system into integrated energy system models: A methodological review. Renewable and Sustainable Energy Reviews 76, 839–856. URL: http://dx.doi.org/10.1016/j.rser.2017.03.090, doi:10.1016/j.rser.2017.03.090.

Conejo, A.J., Baringo, L., Kazempour, J., Siddiqui, A.S., 2016. Investment in electricity generation and transmission: Decision making under uncertainty. doi:10.1007/978-3-319-29501-5.

Cong, H., He, Y., Wang, X., Jiang, C., 2018. Robust optimization for improving resilience of integrated energy systems with electricity and natural gas infrastructures. Journal of Modern Power Systems and Clean Energy 6, 1066–1078. URL: https://doi.org/10.1007/s40565-018-0377-5, doi:10.1007/s40565-018-0377-5.

Deane, J.P., Ó Ciaráin, M., Ó Gallachóir, B.P., 2017. An integrated gas and electricity model of the EU energy system to examine supply interruptions. Applied Energy 193, 479–490. URL: http://dx.doi.org/10.1016/j.apenergy.2017.02.039, doi:10.1016/j.apenergy.2017.02.039.

Dieckhoener, C., 2012. Simulating Security of Supply Effects of the Nabucco and South Stream Projects for the European Natural Gas Market. The Energy Journal 33, 153–181. URL: http://dx.doi.org/10.5547/019, doi:10.5547/019.

Dieckhoener, C., Lochner, S., Lindenberger, D., 2013. European natural gas infrastructure: The impact of market developments on gas flows and physical market integration. Applied Energy 102, 994–1003. doi:10.1016/j.apenergy.2012.06.021.

Egging, R., 2013. Benders decomposition for multi-stage stochastic mixed complementarity problems – applied to a global natural gas market model. European Journal of Operational Research 226, 341–353. URL: https://www.sciencedirect.com/science/article/pii/S0377221712008727, doi:https://doi.org/10.1016/j.ejor.2012.11.024.

Egging, R., Holz, F., 2016. Risks in global natural gas markets: Investment, hedging and trade. Energy Policy 94, 468–479. URL: http://dx.doi.org/10.1016/j.enpol.2016.02.016, doi:10.1016/j.enpol.2016.02.016.

Egging, R., Holz, F., 2019. Global Gas Model: Model and Data Documentation. Technical Report. Deutsches Institut für Wirtschaftsforschung (DIW). Berlin.

Egging, R., Pichler, A., Kalvø, Ø.I., Walle-Hansen, T.M., 2017. Risk aversion in imperfect natural gas markets. European Journal of Operational Research 259, 367–383. URL: http://dx.doi.org/10.1016/j.ejor.2016.10.020, doi:10.1016/j.ejor.2016.10.020.

Energy Community, 2021. Gas 14\ Gas interconnection Poland-Ukraine. URL: https://www.energy-community.org/regionalinitiatives/infrastructure/PLIMA.

ENTSO-G, 2020. TYNDP 2020 Scenario Building Guidelines. Technical Report June. ENTSO-G. URL: https://2020.entsos-tyndp-scenarios.eu.

ENTSOG, 2020. TYNDP 2020 Scenario Report. Technical Report. ENTSOG. URL: https://www.entsog.eu/tyndp#entsog-ten-year-network-development-plan-2020.

Eser, P., Chokani, N., Abhari, R., 2019. Impact of Nord Stream 2 and LNG on gas trade and security of supply in the European gas network of 2030. Applied Energy 238, 816–830. URL: https://doi.org/10.1016/j.apenergy.2019.01.068, doi:10.1016/j.apenergy.2019.01.068.

European Commission, 2014. The European energy security strategy. Technical Report. European Commission. Brussels, Belgium. URL: https://eur-lex.europa.eu/legal-content/EN/TXT/PDF/?uri=CELEX:52014DC0330{&}from=EN, doi:10.4324/9781315455297-11.

European Commission, 2015. The role of gas storage in internal market and in ensuring security of supply. EU publications URL: http://ec.europa.eu/energy/en/studies/, doi:10.2832/568590.

European Commission, 2020. Questions and Answers: The revision of the TEN-E Regulation. URL: https://ec.europa.eu/commission/presscorner/detail/en/QANDA_20_2393.

European Commission, 2021a. Key cross border infrastructure projects. URL: https://ec.europa.eu/energy/topics/infrastructure/projects-common-interest/key-cross-border-infrastructure-projects_en.

European Commission, 2021b. Project of common interest 6.23. PCI fiche: Hungary – Slovenia - Italy interconnection. Technical Report. URL: https://ec.europa.eu/energy/maps/pci_fiches/PciFiche_6.23.pdf.

European Union, 2020. Projects of common interest – Interactive map. URL: https://ec.europa.eu/energy/infrastructure/transparency_platform/map-viewer/main.html.

Eurostat, 2020. European Statistics: Energy, transport and environment indicators. URL: https://ec.europa.eu/eurostat/web/energy/data/database.

Eustream, 2021. Project of common interest (PCI) No. 6.2.1: Poland – Slovakia Interconnection, Eustream (Slovak Gas TSO). URL: https://www.eustream.sk/en_transmission-system/en_pl-sk-interconnector/en_project-of-common-interest-pci.

Flouri, M., Karakosta, C., Kladouchou, C., Psarras, J., 2015. How does a natural gas supply interruption affect the EU gas security? A Monte Carlo simulation. Renewable and Sustainable Energy Reviews 44, 785–796. URL: http://dx.doi.org/10.1016/j.rser.2014.12.029, doi:10.1016/j.rser.2014.12.029.

Fodstad, M., Egging, R., Midthun, K., Tomasgard, A., 2016. Stochastic Modeling of Natural Gas Infrastructure Development in Europe under Demand Uncertainty. The Energy Journal 37. URL: https://doi.org/10.5547/019565, doi:10.5547/019565.

Fulwood, M., 2021. Energy Transition : Modelling the Impact on Natural Gas. Technical Report July. Oxford Institute for Energy Studies. Oxford.

García-Bertrand, R., Mínguez, R., 2017. Dynamic Robust Transmission Expansion Planning. IEEE Transactions on Power Systems 32, 2618–2628. doi:10.1109/TPWRS.2016.2629266, arXiv:1510.03102.

Global Energy Monitor, 2021. Global Fossil Infrastructure Tracker. URL: https://www.gem.wiki/Category:Global{_}Fossil{_}Infrastructure{_}Tracker.

Hauser, P., 2021. Does 'more' equal 'better'? – Analyzing the impact of diversification strategies on infrastructure in the European gas market. Energy Policy 153, 112232. URL: https://www.sciencedirect.com/science/article/pii/S0301421521001014, doi:https://doi.org/10.1016/j.enpol.2021.112232.

Hecking, H., Weiser, F., 2017. Impacts of Nord Stream 2 on the EU natural gas market. Technical Report. ewi Energy Research & Scenarios gGmbH. Cologne.

Holz, F., Richter, P.M., Egging, R., 2016. The Role of Natural Gas in a Low-Carbon Europe : Infrastructure and Supply Security. The Energy Journal 37, 33–59. URL: https://doi.org/10.5547/01956, doi:10.5547/01956.

IEA, 2019. Natural gas information 2019. Technical Report. International Energy Agency. Paris.

Jabr, R.A., 2013. Robust transmission network expansion planning with uncertain renewable generation and loads. IEEE Transactions on Power Systems 28, 4558–4567. doi:10.1109/TPWRS.2013.2267058.

Junne, T., Xiao, M., Xu, L., Wang, Z., Jochem, P., Pregger, T., 2019. How to assess the quality and transparency of energy scenarios: Results of a case study. Energy Strategy Reviews 26, 100380. URL: https://doi.org/10.1016/j.esr.2019.100380, doi:10.1016/j.esr.2019.100380.

Kall, P., Wallace, S.W., 1994. Stochastic Programming. John Wiley and Sons Ltd.

Kiss, A., Selei, A., Tóth, B.T., 2016. A Top-Down Approach to Evaluating Cross-Border Natural Gas Infrastructure Projects in Europe. The Energy Journal 37, 61–79. URL: https://doi.org/10.5547/019565, doi:doi.org/10.5547/019565.

Lappas, N.H., Gounaris, C.E., 2018. Robust optimization for decision-making under endogenous uncertainty. Computers and Chemical Engineering 111, 252–266. doi:10.1016/j.compchemeng.2018.01.006.

Lempert, R.J., Popper, S.W., Bankes, S.C., 2003. Shaping the Next One Hundred Years: New Methods for Quantitative, Long-Term Policy Analysis.. volume 4. RAND. doi:10.5465/amle.2005.19086797.

Lise, W., Hobbs, B.F., 2009. A Dynamic Simulation of Market Power in the Liberalised European Natural Gas Market. The Energy Journal 30, 119–135. URL: www.jstor.org/stable/41323199.

Lochner, S., Bothe, D., 2007. From Russia with gas: an analysis of the Nord Stream pipeline's impact on the European Gas Transmission System with the TIGER-Model.

Lochner, S., Dieckhoener, C., Lindenberger, D., 2010. Model-based Analysis of Infrastructure Projects and Market Integration in Europe with Special Focus on Security of Supply Scenarios. Technical Report May. Institute of Energy Economics at the University of Cologne (EWI). Cologne.

Mínguez, R., García-Bertrand, R., 2016. Robust transmission network expansion planning in energy systems: Improving computational performance. European Journal of Operational Research 248, 21–32. doi:10.1016/j.ejor.2015.06.068, arXiv:1501.05480.

Möst, D., Keles, D., 2010. A survey of stochastic modelling approaches for liberalised electricity markets. European Journal of Operational Research 207, 543–556. URL: http://dx.doi.org/10.1016/j.ejor.2009.11.007, doi:10.1016/j.ejor.2009.11.007.

Neumann, A., Viehrig, N., Weigt, H., 2009. InTraGas - A Stylized Model of the European Natural Gas Network. SSRN Electronic Journal URL: http://www.ivk.tu-dresden.de/die{_}tu{_}dresden/fakultaeten/fakultaet{_}wirtschaftswissenschaften/bwl/ee2/lehrstuhlseiten/ordner{_}publikationen/publications/wp-rm-16{_}neumann{_}etal{_}InTraGas.pdf.

Oil Change International, 2019. Gas and the European Investment Bank: Why New Gas Infrastructure Investment Is Incompatible with Climate Goals. Technical Report. Oil Change International. Washington, D.C.

Pirani, S., Sharples, J., 2020. The Russia-Ukraine gas transit deal: opening a new chapter. Energy Insight 64, 1–9. URL: https://www.oxfordenergy.org/wpcms/wp-content/uploads/2020/02/The-Russia-Ukraine-gas-transit-deal-Insight-64.pdf.

Riepin, I., Müsgens, F., 2022. Seasonal Flexibility in the European Natural Gas Market. The Energy Journal 43. doi:10.5547/01956574.43.1.irie.

Riepin, I., Möbius, T., Müsgens, F., 2021. Modelling uncertainty in coupled electricity and gas systems—is it worth the

effort? Applied Energy 285, 116363. URL: https://www.sciencedirect.com/science/article/pii/S0306261920317426, doi:https://doi.org/10.1016/j.apenergy.2020.116363.

Ruiz, C., Conejo, A., 2015. Robust transmission expansion planning. European Journal of Operational Research 242, 390–401. URL: http://dx.doi.org/10.1016/j.ejor.2014.10.030, doi:10.1016/j.ejor.2014.10.030.

Sesini, M., Giarola, S., Hawkes, A.D., 2020a. The impact of liquefied natural gas and storage on the EU natural gas infrastructure resilience. Energy 209, 118367. URL: https://doi.org/10.1016/j.energy.2020.118367, doi:10.1016/j.energy.2020.118367.

Sesini, M., Giarola, S., Hawkes, A.D., 2020b. The impact of liquefied natural gas and storage on the EU natural gas infrastructure resilience. Energy 209, 118367. URL: https://doi.org/10.1016/j.energy.2020.118367, doi:10.1016/j.energy.2020.118367.

Smeers, Y., 2008. Gas models and three difficult objectives. Core Discussion Paper .

Soyster, A.L., 1973. Programming with Set- Inclusive Constraints and Applications to Inexact Linear Programming. Operations Research 21, 1154–1157. URL: https://doi.org/10.1287/opre.21.5.1154, doi:10.1287/opre.21.5.1154.

Three Seas Iniative, 2019. Priority Interconnection Projects: 2019 Status Report. Technical Report. Three Seas Initiative. Slovenia.

Wallace, S.W., Fleten, S.E., 2003. Stochastic Programming Models in Energy. Handbooks in Operations Research and Management Science 10, 637–677. doi:10.1016/S0927-0507(03)10010-2.

Xunpeng, S., Variam, H.M.P., Tao, J., 2017. Global impact of uncertainties in China's gas market. Energy Policy 104, 382–394. URL: http://dx.doi.org/10.1016/j.enpol.2017.02.015, doi:10.1016/j.enpol.2017.02.015.

Yanikoglu, I., Gorissen, B.L., den Hertog, D., 2019. A survey of adjustable robust optimization. European Journal of Operational Research 277, 799–813. doi:10.1016/j.ejor.2018.08.031.

Yao, L., Wang, X., Qian, T., Qi, S., Zhu, C., 2018. Robust day-ahead scheduling of electricity and natural gas systems via a risk-averse adjustable uncertainty set approach. Sustainability (Switzerland) 10. doi:10.3390/su10113848.

Yue, X., Pye, S., DeCarolis, J., Li, F.G., Rogan, F., Gallachoir, B., 2018. A review of approaches to uncertainty assessment in energy system optimization models. Energy Strategy Reviews 21, 204–217. URL: https://doi.org/10.1016/j.esr.2018.06.003, doi:10.1016/j.esr.2018.06.003.

Zeng, B., Zhao, L., 2013. Solving two-stage robust optimization problems using a column-and- constraint generation method. Operations Research Letters 41, 457–461. URL: http://dx.doi.org/10.1016/j.orl.2013.05.003, doi:10.1016/j.orl.2013.05.003.

Zhao, C., Wang, J., Watson, J.P., Guan, Y., 2013. Multi-stage robust unit commitment considering wind and demand response uncertainties. IEEE Transactions on Power Systems 28, 2708–2717. doi:10.1109/TPWRS.2013.2244231.

Zhou, Y., Wei, Z., Sun, G., Cheung, K.W., Zang, H., Chen, S., 2018. A robust optimization approach for integrated community energy system in energy and ancillary service markets. Energy 148, 1–15. URL: https://doi.org/10.1016/j.energy.2018.01.078, doi:10.1016/j.energy.2018.01.078.

Zhuang, J., Gabriel, S.A., 2008. A complementarity model for solving stochastic natural gas market equilibria. Energy Economics 30, 113–147. doi:10.1016/j.eneco.2006.09.004.

Zwart, G., Mulder, M., 2006. NATGAS: a model of the European natural gas market.

Zwart, G.T., 2009. European Natural Gas Markets : Resource Constraints and Market Power. The Energy Journal 30, 151–165. URL: www.jstor.org/stable/41323201.

Nomenclature

Indices

d	Demands
l	Arcs (pipeline and LNG routes)
n	Nodes
p	Producers
s	Storages
t	Time steps (months)

Sets

Ψ^{l+}	Prospective transmission infrastructure assets (PCIs)
Ψ^{l}	Existing transmission infrastructure assets
Ψ^{T}	Time steps in modelling horizon
Ψ_n^D	Demands located at node n
Ψ_n^P	Producers located at node n
$r(l)/s(l)$	Receiving/sending-end node of the lth arc

Scalars

M	Large scalar value

Parameters

C_d^{LS}	Load-shedding cost of demand d [€/kcm]
C_p^P	Production cost of producer p [€/kcm]
C_l^L	Transport costs across of the lth arc [€/kcm]
$\bar{C}_l^L$	Annualized cost of of the lth arc [€]
$\bar{C}^{\mathrm{I}}$	Annualized investment budget [€]
$\widetilde{G}_{dt}^D$	Reference level of demand d [bcm/m]
$\widetilde{G}_p^P$	Reference capacity of producer p [bcm/a]
$\widehat{G}_{dt}^D$	Max deviation from level of reference demand d [bcm/m]
$\widehat{G}_p^P$	Max deviation from reference capacity of producer p [bcm/m]
$\overline{G}_d^{SI}/\overline{G}_d^{SW}$	Injection/withdrawal capacity of storage mapped to demand d [bcm/m]
$\underline{G}_{dt}^S/\overline{G}_{dt}^S$	Lower/upper bound on working gas volume of storage mapped to demand d [bcm]
η_d^{SI}/η_d^{SW}	Injection/withdrawal efficiency of storage mapped to demand d [%]
E_d^{S0}	Storage level at the first period of modelling horizon [bcm]
Γ^D	Uncertainty budget for demand
Γ^P	Uncertainty budget for supply

Primal Variables

$\overline{g}_{dt}^D$	Uncertain level of demand d [bcm/m]
$\overline{g}_{pt}^P$	Uncertain capacity of producer p [bcm/m]
g_{dt}^{LS}	Load shed by demand d [bcm/m]
g_{lt}^L	Gas transport across lth arc [bcm/m]
g_{pt}^P	Production by producer p [bcm/m]
g_{dt}^{SI}	Gas injection in storage mapped to demand d [bcm/m]
g_{dt}^{SW}	Gas withdrawal from storage mapped to demand d [bcm/m]
wg_{dt}^S	Working gas volume of storage mapped to demand d [bcm]

Binary Variables

x_l^L	Binary investment decision in prospective transmission asset l
z_p^P	Binary variable representing deviation from reference annual supply level $\widetilde{G}_p^P$
z_{dt}^D	Binary variable representing deviation from reference monthly demand level $\widetilde{G}_{dt}^D$

Auxiliary Variables

$\tilde{\lambda}_{nt}$	Auxiliary variable to linearize $z_{d(n)t}^D \cdot \lambda_{nt}$
$\tilde{\phi}_{pt}^P$	Auxiliary variable to linearize $z_p^P \cdot \overline{\phi}_{pt}^P$

Dual Variables

$(\cdot)$	Dual variables are provided after the corresponding equalities or inequalities separated by a colon

Appendix A. Detailed formulation of model application

This Appendix provides the detailed formulation of the transmission expansion planning problem for the European natural gas market.

Appendix A.1. Deterministic model

The transmission expansion planning model for the European natural gas market can be formulated as the following deterministic mixed-integer linear problem (MILP):

$$\min_{\Phi^D} \sum_{l\in\Psi^{L+}} x_l^L \cdot C_l^{IC} + \left(\sum_{pt} g_{pt}^P \cdot C_p^P + \sum_{lt} g_{lt}^L \cdot C_l^L + \sum_{dt} g_{dt}^{LS} \cdot C_d^{LS}\right) \tag{A.1a}$$

subject to

$$x_l^L = \{0,1\} \quad \forall l \in \Psi^{L+} \tag{A.1b}$$

$$\sum_{l\in\Psi^{L+}} x_l^L C_l^{\mathrm{IC}} \leqslant \bar{C}^{\mathrm{I}} \tag{A.1c}$$

$$\sum_{p\in\Psi_n^P} g_{pt}^P + \sum_{d\in\Psi_n^D} (g_{dt}^{SW} - g_{dt}^{SI}) - \sum_{l|s(l)=n} g_{lt}^L + \sum_{l|r(l)=n} g_{lt}^L = \sum_{d\in\Psi_n^D} (\widetilde{G}_{dt}^D - g_{dt}^{LS}) : \lambda_{nt} \quad \forall n, \forall t \tag{A.1d}$$

$$0 \leq g_{lt}^L \leq \overline{G}_{lt}^L : \overline{\phi}_{lt}^L \quad \forall l, \forall t \tag{A.1e}$$

$$0 \leq g_{pt}^P \leq \frac{\widetilde{G}_p^P}{|\Psi^T|} : \overline{\phi}_{pt}^P \quad \forall p, \forall t \tag{A.1f}$$

$$0 \leq g_{dt}^{LS} \leq \widetilde{G}_{dt}^D : \overline{\phi}_{dt}^D \quad \forall d, \forall t \tag{A.1g}$$

$$0 \leq g_{dt}^{SI} \leq \overline{G}_d^{SI} : \overline{\phi}_{dt}^{SI} \quad \forall d, \forall t \tag{A.1h}$$

$$0 \leq g_{dt}^{SW} \leq \overline{G}_d^{SW} : \overline{\phi}_{dt}^{SW} \quad \forall d, \forall t \tag{A.1i}$$

$$wg_{dt}^S = wg_{d,t-1}^S + g_{dt}^{SI}\eta_d^{SI} - \frac{g_{dt}^{SW}}{\eta_d^{SW}} : \mu_{d,t}^S \quad \forall d, \forall t \in \Psi^T \backslash \{t1\} \tag{A.1j}$$

$$wg_{d(t1)}^S = E_d^{S0} + g_{d(t1)}^{SI}\eta_d^{SI} - \frac{g_{d(t1)}^{SW}}{\eta_d^{SW}} : \mu_{d(t1)}^S \quad \forall d, \{t1\} \tag{A.1k}$$

$$\underline{G}_{dt}^S \leq wg_{dt}^S \leq \overline{G}_{dt}^S : \underline{\phi}_{dt}^S, \overline{\phi}_{dt}^S \quad \forall d, \forall t \tag{A.1l}$$

where variables in set $\Phi^D = \{x_l^L; g_{pt}^P; g_d^{LS}; g_{lt}^L; wg_{dt}^S; g_{dt}^{SW}; g_{dt}^{SI}\}$ denote the optimization variables of the deterministic optimization problem. The deterministic optimization problem (A.1) assumes perfect (and optimistic) foresight regarding realizations of natural gas demand and supply levels—$\widetilde{G}_{dt}^D$ and $\widetilde{G}_p^P$, respectively.

The objective function (A.1a) consists of two distinct parts. The first part constitutes investments in infrastructure assets, including pipelines and LNG terminals. Binary variable (x_l^L) represents a discrete investment option of each asset. The second part of the objective function entails the operational costs for existing infrastructure, including production, transportation, and storage costs.

The objective function also includes associated costs for unserved demand. The objective function is subject to a range of constraints. The first such constraint is energy balance (A.1d), which entails the market-clearing condition (i.e., the gas flows entering and exiting a node must balance out). Supply constraints (A.1f)

confine the monthly supply volumes of natural gas in each production node. The transmission constraint (A.1e) limits the monthly volume of natural gas transported via pipelines or LNG arcs. Finally, storage constraints (A.1i - A.1l) limit storage operation and define working gas volume in storage facilities across the time horizon of the model.

Appendix A.2. Adaptive robust optimization model

As noted above, the adaptive robust optimization problem takes the form of the following *min-max-min* problem:

$$\min_{\Phi^1} \sum_{l \in \Psi^{L+}} x_l^L \cdot C_l^{IC} + \max_{\Phi^2 \in \Omega} \min_{\Phi^3 \in \Xi(\cdot)} \left[\sum_t \left(\sum_p g_{pt}^P \cdot C_p^P + \sum_l g_{lt}^L \cdot C_l^L + \sum_d g_{dt}^{LS} \cdot C_d^{LS} \right) \right] \tag{A.2a}$$

subject to

$$\text{Constraints (A.1b) - (A.1c)} \tag{A.2b}$$

where variables in sets $\Phi^1 = \left\{x_l^L, \forall l \in \Psi^{L+}\right\}$, $\Phi^2 = \left\{\overline{g}_{dt}^D; \overline{g}_{pt}^P\right\}$, and $\Phi^3 = \left\{g_{pt}^P; g_d^{LS}; g_{lt}^L; wg_{dt}^S; g_{dt}^{SW}; g_{dt}^{SI}\right\}$ denote the optimization variables of the first, second, and third level optimizations problems, respectively. The three-tiered formulation incorporates the following nested optimization problems:

1. The first level involves the determination of cost-optimal expansion decisions (i.e., the variables in set Φ^1 that correspond to investments in pipelines and LNG infrastructure).
2. The second level corresponds to unfortunate realizations of uncertainty variables represented by uncertainty sets (i.e., variables in set Φ^2).
3. The third level consists of corrective dispatch decisions, made in response to perturbations elicited by the first- and second-level decisions, that ensure a feasible solution (i.e., variables in set Φ^3 that correspond to the production, transportation, and storage of natural gas as well as, if necessary, the shedding of demand).

In problem (A.2), Ω and Ξ represent the uncertainty and feasibility sets, respectively.

Appendix A.3. Uncertainty sets

As explained in section 3.1.2, uncertainty in the demand and supply of natural gas is expressed by constructing confidence bounds around the respective decision variables. This is implemented in the model

using the following cardinality-constrained uncertainty set formulation (Baringo et al., 2020):

$$\Omega = \Big\{ \overline{g}^D_{dt} = \widetilde{G}^D_{dt} + z^D_{dt} \cdot \widehat{G}^D_{dt} \quad \forall d, \forall t \tag{A.3a}$$

$$\overline{g}^P_p = \widetilde{G}^P_p - z^P_p \cdot \widehat{G}^P_p \quad \forall p \tag{A.3b}$$

$$\sum_{d \in D, t \in T} z^D_{dt} \leq \Gamma^D \tag{A.3c}$$

$$\sum_{p \in P} z^P_p \leq \Gamma^P \tag{A.3d}$$

$$z^D_{dt} \in \{0,1\} \quad \forall d, \forall t \tag{A.3e}$$

$$z^P_p \in \{0,1\} \quad \forall p \} \tag{A.3f}$$

Appendix A.4. Feasibility sets

Given the first- and second-level decision variables, the set Ξ models the feasible space of third-level optimization problem: $\Xi(g^P_{pt}; g^{LS}_d; g^L_{lt}; wg^S_{st}; g^{SW}_{st}; g^{SI}_{st}) =$

$$\big\{ \Phi^3 :$$

$$\sum_{p \in \Psi^P_n} g^P_{pt} + \sum_{d \in \Psi^D_n} (g^{SW}_{dt} - g^{SI}_{dt}) - \sum_{l|s(l)=n} g^L_{lt} + \sum_{l|r(l)=n} g^L_{lt} =$$

$$\sum_{d \in \Psi^D_n} (\overline{g}^D_{dt} - g^{LS}_{dt}) : \lambda_{nt} \quad \forall n, \forall t \tag{A.4a}$$

$$0 \leq g^L_{lt} \leq \overline{G}^L_{lt} : \overline{\phi}^L_{lt} \quad \forall l, \forall t \tag{A.4b}$$

$$0 \leq g^P_{pt} \leq \overline{g}^P_{pt} : \overline{\phi}^P_{pt} \quad \forall p, \forall t \tag{A.4c}$$

$$0 \leq g^{LS}_{dt} \leq \widetilde{G}^D_{dt} : \overline{\phi}^D_{dt} \quad \forall d, \forall t \tag{A.4d}$$

$$0 \leq g^{SI}_{dt} \leq \overline{G}^{SI}_d : \overline{\phi}^{SI}_{st} \quad \forall d, \forall t \tag{A.4e}$$

$$0 \leq g^{SW}_{dt} \leq \overline{G}^{SW}_d : \overline{\phi}^{SW}_{st} \quad \forall d, \forall t \tag{A.4f}$$

$$wg^S_{dt} = wg^S_{d,t-1} + g^{SI}_{dt} \eta^{SI}_d - \frac{g^{SW}_{dt}}{\eta^{SW}_d} : \mu^S_{d,t} \quad \forall d, \forall t \in \Psi^T \backslash \{t1\} \tag{A.4g}$$

$$wg^S_{d(t1)} = E^{S0}_d + g^{SI}_{d(t1)} \eta^{SI}_d - \frac{g^{SW}_{d(t1)}}{\eta^{SW}_d} : \mu^S_{d(t1)} \quad \forall d, \{t1\} \tag{A.4h}$$

$$\underline{G}^S_{dt} \leq wg^S_{dt} \leq \overline{G}^S_{dt} : \phi^S_{dt} \quad \forall d, \forall t \tag{A.4i}$$

$$\}$$

The associated dual variables for the respective constraints are provided after the colon in each equation.

Appendix A.5. Solution procedure

We use the column-and-constraint generation algorithm detailed in section 3.2 to iteratively solve the master and subproblem of the ARO model. A formulation of the master and subproblem in the explicit form is described in the following.

Appendix A.5.1. Master problem

The master problem at iteration v is as follows:

$$\min_{\Phi^{\mathrm{M}}} \sum_{l\in\Psi^{L+}} x_l^L \cdot C_l^{IC} + \theta \tag{A.5a}$$

subject to

Constraints (A.1b) - (A.1c)

$$\theta \geqslant \left[\sum_t \left(\sum_p g_{ptv'}^P \cdot C_p^P + \sum_l g_{ltv'}^L \cdot C_l^L + \sum_d g_{dtv'}^{LS} \cdot C_d^{LS}\right)\right], \quad \forall v' \leqslant v \tag{A.5b}$$

$$\sum_{p\in\Psi_n^P} g_{ptv'}^P + \sum_{d\in\Psi_n^D} (g_{dt}^{SW} - g_{dt}^{SI}) - \sum_{l|s(l)=n} g_{ltv'}^L + \sum_{l|r(l)=n} g_{ltv'}^L = \sum_{d\in\Psi_n^D} (\overline{g}_{dt}^{D(v')} - g_{dtv'}^{LS}) \quad \forall n, \forall t, \forall v' \leqslant v \tag{A.5c}$$

$$0 \leqslant g_{ltv'}^L \leqslant \overline{G}_{lt}^L \quad \forall l, \forall t, \forall v' \leqslant v \tag{A.5d}$$

$$0 \leqslant g_{ptv'}^P \leqslant \frac{\overline{g}_p^{P(v')}}{|\Psi^T|} \quad \forall p, \forall t, \forall v' \leqslant v \tag{A.5e}$$

$$0 \leqslant g_{dtv'}^{LS} \leqslant \widetilde{G}_{dt}^D \quad \forall d, \forall t, \forall v' \leqslant v \tag{A.5f}$$

$$0 \leqslant g_{dtv'}^{SI} \leqslant \overline{G}_d^{SI} \quad \forall d, \forall t, \forall v' \leqslant v \tag{A.5g}$$

$$0 \leqslant g_{dtv'}^{SW} \leqslant \overline{G}_d^{SW} \quad \forall d, \forall t, \forall v' \leqslant v \tag{A.5h}$$

$$wg_{dtv'}^S = wg_{d,t-1,v'}^S + g_{dtv'}^{SI} \cdot \eta_d^{SI} - \frac{g_{dtv'}^{SW}}{\eta_d^{SW}} \quad \forall d, \forall t \in \Psi^T \backslash \{t1\}, \forall v' \leqslant v \tag{A.5i}$$

$$wg_{d(t1)v'}^S = E_d^{S0} + g_{d(t1)v'}^{SI} \cdot \eta_d^{SI} - \frac{g_{d(t1)v'}^{SW}}{\eta_d^{SW}} \quad \forall d, \{t1\}, \forall v' \leqslant v \tag{A.5j}$$

$$\underline{G}_{dt}^S \leqslant wg_{dtv'}^S \leqslant \overline{G}_{dt}^S \quad \forall d, \forall t, \forall v' \leqslant v \tag{A.5k}$$

where set $\Phi^{\mathrm{M}} = \left\{\Phi^1; \theta; g_{ptv'}^{\mathrm{P}}; g_{dtv'}^{\mathrm{LS}}; g_{ltv'}^{\mathrm{L}}; wg_{dtv'}^{\mathrm{S}}; g_{dtv'}^{\mathrm{SI}}; g_{dtv'}^{\mathrm{SW}}\right\}$ are the optimization variables of master problem (A.5).

Appendix A.5.2. Subproblem

At each iteration v, master problem (A.5) yields the expantion decisions. The subproblem formulated below takes these decisions as input and determines the worst-case uncertainty realization:

$$\max_{\Phi^2\in\Omega} \quad \min_{\Phi^3\in\Xi(\cdot)} \left[\sum_t \left(\sum_p g_{pt}^P \cdot C_p^P + \sum_l g_{lt}^L \cdot C_l^L + \sum_d g_{dt}^{LS} \cdot C_d^{LS}\right)\right] \tag{A.6}$$

Subproblem (A.6) is a bilevel problem in which the lower-level problem is continuous and linear on its decisions variables. Thus, we follow Baringo et al. (2020) and replace the lower-level problem by its dual form. Furthermore, we can replace the objective function of the subproblem by the dual objective function

using the strong duality theorem. This allows formulating the subproblem as the single-level problem:

$$\max_{\Phi^2,\Phi^3}$$

$$\sum_t \Bigg[\sum_{d\in\Psi_n^D} (\widetilde{G}_{dt}^D \lambda_{n(d)t} + \widehat{G}_{dt}^D \widetilde{\lambda}_{n(d)t}) + \sum_{l\in\Psi^L} -\overline{G}_{lt}^L \overline{\phi}_{lt}^L + \sum_{l\in\Psi^{L+}} -\overline{G}_{lt}^L X_l^{L(v)} \overline{\phi}_{lt}^L$$

$$+ \sum_p (-\frac{\widetilde{G}_p^P}{|\Psi^T|}\overline{\phi}_{pt}^P + \frac{\widehat{G}_p^P}{|\Psi^T|}\tilde{\phi}_{pt}^P) + \sum_d (-\overline{G}_d^{SI}\overline{\phi}_{dt}^{SI} - \overline{G}_d^{SW}\overline{\phi}_{dt}^{SW} + \underline{G}_{dt}^S \underline{\phi}_{dt}^S - \overline{G}_d^S \overline{\phi}_{dt}^S)$$

$$+ \sum_d -\widetilde{G}_d^D \overline{\phi}_d^D \Bigg] + \sum_d \mu_{d,\{t1\}}^S E_d^{S0} \tag{A.7a}$$

subject to

$$\overline{g}_{dt}^D = \widetilde{G}_{dt}^D + z_{dt}^D \cdot \widehat{G}_{dt}^D \quad \forall d, \forall t \tag{A.7b}$$

$$\overline{g}_p^P = \widetilde{G}_p^P - z_p^P \cdot \widehat{G}_p^P \quad \forall p \tag{A.7c}$$

$$\sum_{d\in D, t\in T} z_{dt}^D \le \Gamma^D \tag{A.7d}$$

$$\sum_{p\in P} z_p^P \le \Gamma^P \tag{A.7e}$$

$$\lambda_{n(p)t} - \overline{\phi}_{pt}^P - c_p^P \le 0 \quad \forall p, \forall t \tag{A.7f}$$

$$\lambda_{n(d)t} - \overline{\phi}_{dt}^D - c_d^{LS} \le 0 \quad \forall d, \forall t \tag{A.7g}$$

$$-\lambda_{n(s(l))t} + \lambda_{n(r(l))t} - \overline{\phi}_{lt}^L - c_l^L \le 0 \quad \forall l \in \Psi^L \cup \Psi^{L+} | X_l^{L(v)} = 1, \forall t \tag{A.7h}$$

$$\lambda_{n(d)t} - \overline{\phi}_{dt}^{SW} - \frac{1}{\eta_d^{SW}} \cdot \mu_{dt}^S \le 0 \quad \forall d, \forall t \tag{A.7i}$$

$$-\lambda_{n(d)t} - \overline{\phi}_{dt}^{SI} + \eta_d^{SI} \mu_{dt}^S \le 0 \quad \forall d, \forall t \tag{A.7j}$$

$$-\mu_{dt}^S + \mu_{d,t+1}^S + \underline{\phi}_{dt}^S - \overline{\phi}_{dt}^S = 0 \quad \forall d, \forall t = 1, ...\Psi_{|\Psi^T|}^T - 1 \tag{A.7k}$$

$$-\mu_{d,t}^S + \underline{\phi}_{d,t}^S - \overline{\phi}_{d,t}^S = 0 \quad \forall s, \forall t = \Psi_{|\Psi^T|}^T \tag{A.7l}$$

$$\overline{\phi}_{pt}^P \ge 0 \quad \forall p, \forall t \tag{A.7m}$$

$$\overline{\phi}_{dt}^D \ge 0 \quad \forall d, \forall t \tag{A.7n}$$

$$\overline{\phi}_{lt}^L \ge 0 \quad \forall l \in \Psi^L, \forall t \tag{A.7o}$$

$$\overline{\phi}_{lt}^L \ge 0 \quad \forall l \in \Psi^{L+} | X_l^{L(v)} = 1, \forall t \tag{A.7p}$$

$$\overline{\phi}_{dt}^{SW}, \overline{\phi}_{dt}^{SI}, \underline{\phi}_{dt}^S, \overline{\phi}_{dt}^S \ge 0 \quad \forall d, \forall t \tag{A.7q}$$

$$\mu_{dt}^S \quad free \quad \forall d, \forall t \tag{A.7r}$$

$$\lambda_{nt} \quad free \quad \forall n, \forall t \tag{A.7s}$$

$$z_{dt}^D \in \{0,1\} \quad \forall d, \forall t \tag{A.7t}$$

$$z_p^P \in \{0,1\} \quad \forall p \tag{A.7u}$$

865

Note that to omit a MINLP formulation, we use a linearization technique addressing the bilinear terms

$\lambda_{n(d)t} \cdot \overline{g}^{D}_{dt}$ and $\overline{\phi}^{P}_{pt} \cdot \overline{g}^{P}_{pt}$ in the objective function of the problem (A.7). The following constraints are added to the problem rendering the subproblem into the equivalent MILP problem:

$$(-M) \cdot z^{D}_{d(n)t} \leq \tilde{\lambda}_{nt} \leq (M) \cdot z^{D}_{d(n)t} \tag{A.8a}$$

$$(-M) \cdot (1 - z^{D}_{d(n)t}) \leq \lambda_{nt} - \tilde{\lambda}_{nt} \leq (M) \cdot (1 - z^{D}_{d(n)t}) \tag{A.8b}$$

$$(-M) \cdot z^{P}_{p} \leq \tilde{\phi}^{P}_{pt} \leq (M) \cdot z^{P}_{p} \tag{A.8c}$$

$$(-M) \cdot (1 - z^{P}_{p}) \leq \overline{\phi}^{P}_{pt} - \tilde{\phi}^{P}_{pt} \leq (M) \cdot (1 - z^{P}_{p}) \tag{A.8d}$$

Appendix B. Demand and Supply Uncertainty Budgets

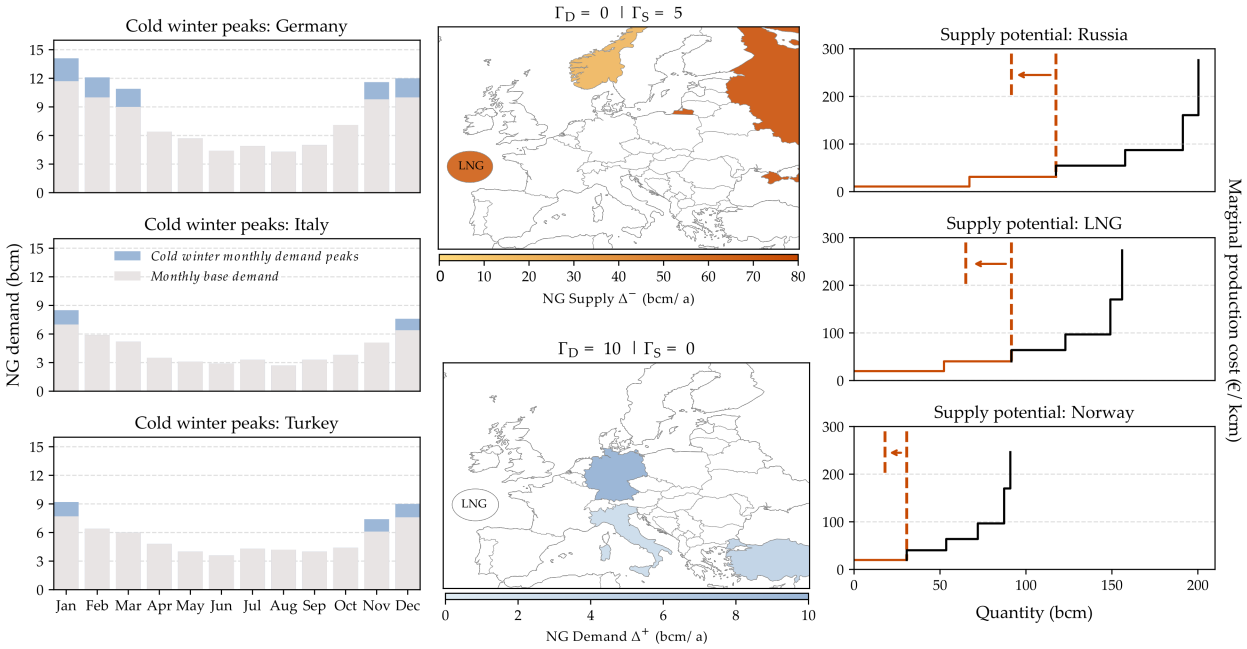

Figure B.11: Illustrative example of the realisation of the worst-case demand and supply realisations subject to uncertainty budgets [Γ], source: Source: Authors' illustration

Appendix C. Projects of Common Interests included in the model

No.	PCI project	Capacity (bcm/a)	Start year	Estimated CAPEX* (MEUR)	Financing* from CEF** & EC with FID (MEUR)	Status
1	Poland-Lithuania Interconnector	2.4 (PL-LT) 1.9 (LT-PL)	2022-2023	558	276	Under Construction
2	Baltic Pipe Interconnector	3.1 (PL-DK) 10.4 (DK-PL)	2022	784	267	Under Construction
3	Latvia-Lithuania Interconnector	1.9 (LT-LV) 2.0 (LV-LT)	2023	37	-	Proposed
4	Bulgaria-Serbia Interconnector	1.8 (BG-SB) 0.2 (SB-BG)	2022	487	77	Under Construction
5	Eastring Pipeline (a)	4.4 (RO-HU) 4.4 (HU-RO)	2025	547	-	Proposed
6	Eastring Pipeline (b)	3.3 (TR-BG) 3.3 (BG-TR)	2025	200	-	Proposed
7	Hungary-Slovenia-Italy Interconnector	1.4 (HU-SI) 1.4 (SI-HU)	2025	104	-	Proposed
8	Croatia-Slovenia-Austria Interconnector	2.7 (AT-SI) 5.5 (SI-AT)	2023	218	-	Proposed
9		5.0 (SI-HR) 5.0 (HR-SI)	2023	218		Proposed
10	Slovakia-Hungary Interconnector***	3.8 (HU-SK) 1.0 (SK-HU)	2022	138	-	Proposed
11	Poland-Slovakia Interconnector	4.7 (PL-SK) 5.7 (SK-PL)	2021	287	107	Under Construction
12	Greece-Bulgaria Interconnector	5.0 (GR-BG) 5.0 (BG-GR)	2021	287	-	Proposed
13	Poseidon Gas Pipeline	14.0 (GR-IT) 14.0 (IT-GR)	2022-2025	2096	-	Proposed
14	Shannon LNG Terminal	2.8 (IE)	2022	500	-	Proposed
15	Krk LNG Terminal	2.6 (HR)	2021	234	107	In operation
16	Baltic Sea Coast LNG Terminal	4.0 (PL)	2022	196	-	Proposed
17	Alexandroupolis LNG Terminal	6.1 (GR)	2023	382	-	Proposed

* Information on PCI project is collected from www.gem.wiki web-page unless stated otherwise (Status: June 2021)
** The Connecting Europe Facility (CEF) https://ec.europa.eu/inea/en/connecting-europe-facility
*** PCI status pertains to the expansion of the existing interconnector

Appendix D. Literature Review of Natural Gas Models and Representation of Uncertainty

Author/year	Problem type	Uncertainty addressed
Zwart and Mulder (2006)	deterministic	supply, demand, capital costs
Lochner and Bothe (2007)	deterministic	pipeline capacities
Zhuang and Gabriel (2008)	stochastic	LTCs, spot market
Lise and Hobbs (2009)	deterministic	-
Zwart (2009)	deterministic	resource constraints
Neumann et al. (2009)	deterministic	supply, demand, infrastructure
Lochner et al. (2010)	deterministic	supply, demand, infrastructure
Abada and Massol (2011)	deterministic	supply interruptions
Abada and Jouvet (2012)	stochastic	demand
Dieckhoener (2012)	deterministic	infrastructure projects
Dieckhoener et al. (2013)	deterministic	demand, supply, pipeline capacities
Egging (2013)	stochastic	production, market structure
Chyong and Hobbs (2014)	deterministic	demand, South Stream pipeline, transit fees
Flouri et al. (2015)	Monte Carlo simulation	supply disruptions
Egging and Holz (2016)	stochastic	demand, supply disruptions, resource basis
Fodstad et al. (2016)	stochastic	demand
Holz et al. (2016)	deterministic	demand
Kiss et al. (2016)	deterministic	infrastructure projects
Baltensperger et al. (2017)	deterministic	LNG supply, supply disruptions
Hecking and Weiser (2017)	deterministic	LNG supply, Nord Stream 2 pipeline
Egging et al. (2017)	stochastic	shale gas exploration
Xunpeng et al. (2017)	deterministic	shale gas production, demand
Deane et al. (2017)	deterministic	supply disruptions
Abrell et al. (2019)	deterministic	infrastructure projects
Eser et al. (2019)	deterministic	infrastructure projects
Sesini et al. (2020a)	stochastic	supply disruptions
Sesini et al. (2020b)	deterministic	LNG supply, Nord Stream 2 pipeline
Hauser (2021)	stochastic	demand, supply disruptions
Riepin et al. (2021)	stochastic	demand

Table D.1: Overview of natural gas models and their respective representation of uncertainty